Aus dem Institut für Molekulare Onkologie

(Prof. Dr. med. M. Dobbelstein)

der Medizinischen Fakultät der Universität Göttingen

Cancer cell death by mitotic failure upon combined kinase inhibition

INAUGURAL-DISSERTATION

zur Erlangung des Doktorgrades

der Medizinischen Fakultät der

Georg-August-Universität zu Göttingen

vorgelegt von

Antonia Kleeberg

aus

Schleswig

Göttingen 2021

Dekan:	Prof. Dr. med. W. Brück

Betreuungsausschuss

Betreuer/in	Prof. Dr. med. M. Dobbelstein
Ko-Betreuer/in:	Prof. Dr. med. E. Heßmann

Prüfungskommission

Referent/in	Prof. Dr. med. M. Dobbelstein
Ko-Referent/in:	Prof. Dr. med. E. Heßmann
Drittreferent/in:	Prof. Dr. hum. biol. Margarete Schön

Datum der mündlichen Prüfung: 15.06.2022

Hiermit erkläre ich, die Dissertation mit dem Titel "Cancer cell death by mitotic failure upon combined kinase inhibition" eigenständig angefertigt und keine anderen als die von mir angegebenen Quellen und Hilfsmittel verwendet zu haben.

Göttingen, den 04.11.2021 ……

(Unterschrift)

Inhaltsverzeichnis

List of figures

List of tables

Abbreviations

APS	Ammonium persulfate
AURKB	Aurora kinase B
ATM	Ataxia telangiectasia mutated
ATR	Ataxia telangiectasia and Rad3-related
BCA	Bicinchoninic acid
BSA	Bovine serum albumin
CDKs	Cyclin-dependent kinases
CFI	CFI-400945
CldU	5-Chloro-2'-deoxyuridine
ddH_2O	Double-distilled water
DMEM	Dulbecco's modified eagle medium
DMSO	Dimethyl sulfoxide
EDTA	Ethylenediaminetetraacetic acid
EGFR	Epidermal growth factor receptor
FACS	Fluorescence-activated cell sorting
G1/G2 phase	Gap 1/2 phase
HRP	Horseradish peroxidase
IdU	5-Iodo-2'-deoxyuridine
IF	Immunofluorescence
LPF3000	Lipofectamine 3000
MK2/MAPKAPK2	Mitogen-activated protein kinase-activated protein kinase 2
PBS	Phosphate buffered saline
PCNT	Pericentrin
PLK4	Polo-like kinase 4

S phase	Synthesis phase
SAC	Spindle-assembly checkpoint
SDS-PAGE	Sodium dodecyl sulphate polyacrylamide gel electrophoresis
TEMED	Tetramethylethylenediamine

1 Introduction

Cancer represents one of the most challenging diseases of our time. Despite all progress being made in medical research, with almost nine million deaths in 2016, cancer was the second most frequent cause of death worldwide (Roth et al. 2018).

Among the heterogeneous group of cancer diseases, lung cancer tends to be one of the most aggressive ones: Even though lung cancer constitutes the fourth most common form of cancer by prevalence, it is the leading cause of cancer-related death (Roth et al. 2018).

There are several different cancer therapy options today and a lot of progress has been made in the past decades. Traditional options reach from operative strategies over radiation therapy to chemotherapeutics. These therapies are commonly recommended in European cancer therapy guidelines, for example, surgery in non-metastatic colon carcinoma or chemotherapy in Hodgkin lymphoma (Labianca et al. 2013; Eichenauer et al. 2018). Yet, they are limited in their outcome: Chemotherapy targets fast-dividing cells in a very non-specific manner and thus causes severe side-effects. Radiation therapy and surgery may provide a good reduction of the primary tumor but cannot always target all metastases.

A new field that has been established in the past years includes therapies targeting cancer cells more specifically. Among these there are pharmacological inhibitors (small molecule inhibitors) and monoclonal antibodies that are targeted against receptors, such as EGFR-tyrosine kinase inhibitors used in non-small cell lung carcinoma.

Although much research has been done in this field, cancer and particularly lung cancer remains among the most harmful predators of mankind. Many more ideas will have to come up in order to be able to combat cancer one day.

1.1 The cell cycle

To be able to proliferate, cells undergo a certain process of alternating cell growth, cell rest and cell division, commonly referred to as the cell cycle. This cycle consists of three parts: interphase, mitosis and cytokinesis. In interphase, cells are being prepared for mitosis and cell division: the genome and cell organelles are being duplicated. During mitosis, the genetic information that has been duplicated before is being separated into two new nuclei. Cytokinesis completes the cell cycle by mediating the final division of the cell, generating two new daughter cells (Cooper and Hausman 2015).

In healthy tissue, most cells are in interphase, as interphase accounts for about 95% of the time of the normal cell cycle. Interphase can be subdivided into G1 (Gap 1), S (Synthesis) and G2 (Gap 2) phase. G1 phase serves as a preliminary stage for the following S phase, ensuring that all protein necessary for replication is available in the cell. In the S phase, DNA replication takes place. In the G2 phase, replication errors are being repaired by various DNA repair machineries (Cooper and Hausman 2015).

Not always, DNA replication errors may be repaired during the normal progression of the cell cycle. This can be imagined like trying to repair a train while it is moving: Broken seats inside the train may well be repaired while it is moving – a broken motor may not. When the motor is broken, the train will need to stop until the motor is repaired. In analogy to this, when DNA replication errors in a cell are too severe to be repaired in G2 phase, cell cycle needs to be halted. This is when cell cycle regulation by checkpoint kinases becomes important.

1.1.1 Cell cycle regulation and checkpoint kinases

Cell cycle regulation enables cells to stop the normal progression in cell cycle, i.e., to halt the cell cycle at a certain point. When the cell cycle is halted, there are different ways to deal with replication errors: Either the errors get repaired, or the cell undergoes cell death if the errors are too severe to be repaired. If none of these mechanisms is successful, the cell continues dividing but carries mutations.

For the regular continuation of the cell cycle, previous steps of the cycle must be completed in a proper way. The prerequisites for continuation are manifold and range from the availability of nutrients over the correct formation of the spindle to

DNA integrity. The occasions where these requirements are being checked are called checkpoints (Yasutis and Kozminski 2013).

The minimal set of molecules necessary for coordinating the cell cycle proceeding at checkpoints are Cyclins and Cyclin-dependent kinases (CDKs) (Coudreuse and Nurse 2010). CDKs are being activated by Cyclins and consequently phosphorylate other proteins which initiate the progression of the cell cycle (Morgan 1997).

If, however, DNA damage is present at one of the checkpoints or essential steps have not been completed, there are several ways for the cell to transiently stop the cell cycle from proceeding and either induce apoptosis or DNA damage repair. The kinases mediating this damage response are called checkpoint kinases (Walworth 2000).

Three major signaling pathways mediate the checkpoint response: ATR/Chk1 (Ataxia telangiectasia and Rad3-related/Checkpoint kinase 1), ATM/Chk2 (Ataxia telangiectasia mutated/Checkpoint kinase 2) and p38/MK2 (Mitogen-activated protein kinase-activated protein kinase 2, MAPKAP2) (Bartek et al. 2004; Manke et al. 2005). Eventually, they culminate in the inhibition of Cdc25 phosphatases, a process which leads to lacking activation of Cyclin/CDK complexes, as a result stopping the cell cycle from proceeding (Donzelli and Draetta 2003).

For different kinds of stressors, distinct pathways are activated. For example, when encountering DNA double-strand breaks (DSBs), the p38/MK2 pathway is activated like it is displayed in **Figure 1**: Activated MK2 phosphorylates Cdc25B which leads to binding of the protein 14-3-3. Through the binding of 14-3-3, Cdc25B is being transported out of the nucleus so that it cannot dephosphorylate the CDK1/Cyclin B complex. The cell is arrested in G2 phase (Thornton and Rincon 2009; Reinhardt et al. 2010).

This kind of fault management is utterly important because it is essential for cells that replication happens in a very well-sorted and precise manner. If the other way around, a cell continues to divide despite mistakes in the genome, mutations arise. Subsequently, chromosome missegregation might take place with incorrect numbers of chromosomes in daughter cells. These aberrant chromosome numbers lead to cell death or, if the respective cell succeeds to proliferate further, eventually drive tumorigenesis (Levine et al. 2017).

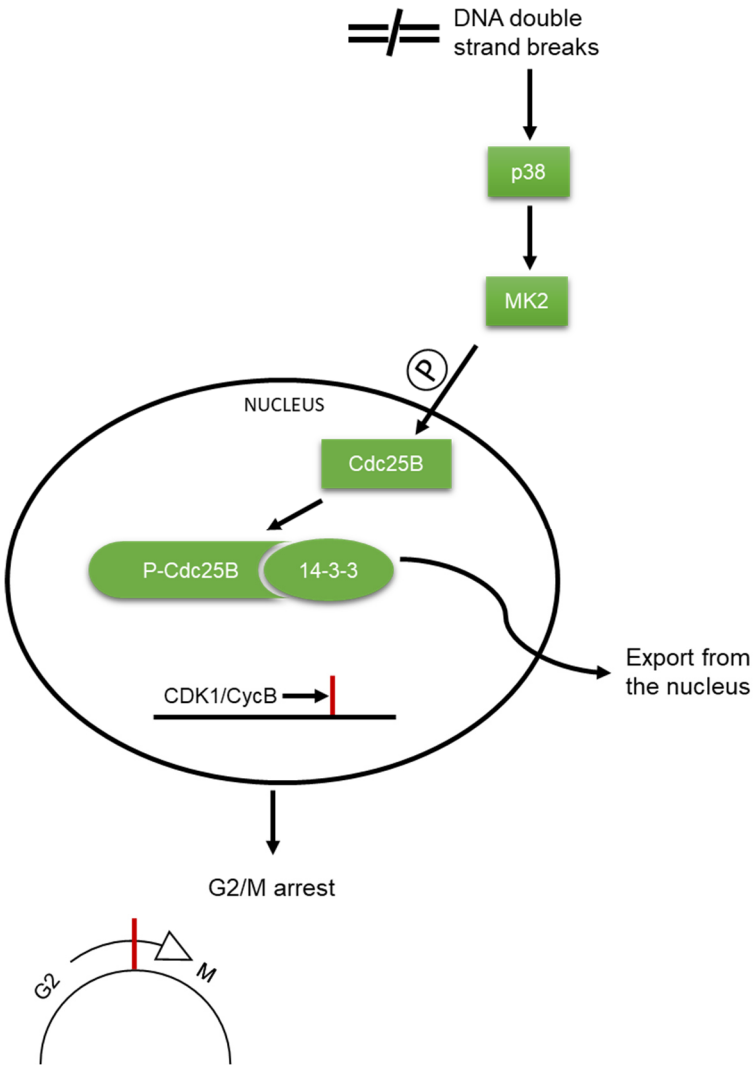

Figure 1: The p38-MK2 pathway in response to DNA double-strand breakage. DNA double-strand breakage leads to activation of the p38-MK2 pathway which eventually causes a G2/M arrest.

1.1.2 Replication and replicative stress

It is necessary to duplicate DNA once per cell cycle to have sufficient DNA content for both daughter cells. I outlined above that so-called checkpoints are mechanisms of control that ensure proper cell division by arresting the cell cycle between cell cycle phases. But what happens if the DNA machinery encounters DNA damage which has just occurred during DNA replication?

When DNA polymerases encounter DNA damage, they temporarily cease their work. This is a phenomenon known as fork stalling. Similar to other checkpoints, with the fork stalled, the damage either will be repaired or the replication apparatus will be separated from the replication fork. Upon separation from its replication apparatus, the fork collapses (Dobbelstein and Sørensen 2015).

However, when forks stall and the polymerases cease their work, other enzymes, the so-called replicative MCM (minichromosome maintenance) helicases, keep working. Hence, single-stranded DNA (ssDNA) accumulates. This ssDNA is coated by Replication Protein A (RPA), leading to activation of ATR and phosphorylation of H2AX, among others. These signaling cascades act as protectors from fork collapsing (Dobbelstein and Sørensen 2015).

Furthermore, stalled forks often experience DNA cleavage by endonucleases. This leads to the formation of DSBs and the subsequent activation of p38-MK2 pathways as explained in 1.1.1. The pattern of *DNA damage in S phase – fork stalling – activation of certain signaling cascades* is often referred to as replicative stress (Dobbelstein and Sørensen 2015).

Due to several reasons, replicative stress is a feature often found in tumor cells. These reasons include the increased proliferation rate of cancer cells and the activation of certain oncogenes leading to a faster progression through cell cycle. A fast progression through cell cycle renders cells more prone to DNA damage in S phase and consequently leads to increased replicative stress. This knowledge can be used to “exploit” replicative stress in the therapy of cancer (Dobbelstein and Sørensen 2015).

Traditionally, the thought behind chemotherapy is to stop the proliferation of cancer cells by preventing them from replicating their DNA. The novel approach is to even push cancer cells towards DNA replication to enhance replicative stress

and by this, to make them run into mitotic suicide. This can be achieved by checkpoint kinase inhibitors (Collins and Garrett 2005).

Many conventional chemotherapeutics already do enhance replicative stress on cells (for example nucleotide analogues), but in a very non-selective way. The aim today is to exploit replicative stress in cancer therapy by using more selective, more targeted therapies. As cancer cells show enhanced replicative stress, the idea is to directly target pathways of the replicative stress response to address cancer cells more specifically (Dobbelstein and Sørensen 2015).

1.1.3 Mitosis

After replication has taken place (S phase) and replication mistakes have been corrected (G2 phase), cells enter mitosis to carry out the separation of the nucleus. The crucial cell organelle for accomplishing this step is the centrosome.

1.1.3.1 Centrosomes

Centrosomes are non-membranous cell organelles showing a variety of functions in the field of cell shape, cell motility and cell division. As their main function, centrosomes organize the mitotic spindle of mammalian cells. Centrosomes are built up out of two centrioles standing orthogonally to each other. The centrioles themselves are made from several microtubules. They are surrounded by the pericentriolar matrix, a structure of proteins that belong to the centrosomes and regulate the process of centrosomal duplication (Dammermann et al. 2004).

Centrosomes need to duplicate once per cell cycle to constitute the two poles of the mitotic spindle in M (mitotic) phase. During mitosis, the two centrosomes migrate to opposite poles of the cell to tear the sister chromatids away from each other. After a successful cell division, each daughter cell has one centrosome.

Centrosomal duplication, just like DNA replication, takes place in S phase and is a process tightly regulated by many proteins. This tight regulation is necessary to avoid chromosomal missegregation which might lead to the formation of cells carrying supernumerary chromosomes, a condition that is discussed to be linked to tumorigenesis (Nam et al. 2015; Levine et al. 2017).

1.1.3.2 PLK4

One protein that is utterly important in regulating centrosomal duplication is PLK4 (Polo-like kinase 4). PLK4 belongs to the family of serine/threonine protein kinases, transferring phosphate groups from ATP to substrates (proteins).

PLK4, which is referred to as a “master regulator of centrosome duplication” (Nakamura et al. 2013; Moyer et al. 2015), initiates centriole biogenesis in the S phase (Habedanck et al. 2005; Nakamura et al. 2013). Correspondingly, PLK4 depletion leads to centrosomal depletion whilst PLK4 overexpression leads to centrosomal amplification (Wong et al. 2015; Moyer et al. 2015). PLK4 activity needs to be tightly regulated to avoid centrosomal amplification.

According to Nakamura et al. (2013), PLK4 also plays a role in the cellular stress response (see **Figure 2**): When cells experience stress, the so-called SAPKKKs (stress-activated protein kinase kinase kinases) are activated. Subsequently, both the pro-apoptotic SAPKs (stress-activated protein kinases, for example, MKK4) and the anti-apoptotic PLK4 are activated.

PLK4 provides a pro-survival signal to the cell, giving it time for repair mechanisms. This pathway is being regulated by two proteins: p53 and MKK4 (a SAPK, see above). P53 inhibits PLK4 activity in the late phase of stress response, thereby providing a time-limit for repair mechanisms. MKK4 inhibits PLK4-mediated centrosome duplication and therefore provides pro-apoptotic signals.

In healthy cells that experience stress, SAPKKKs activate PLK4 and MKK4 simultaneously. PLK4 acts anti-apoptotic and drives centriole duplication. MKK4 inhibits centriole overduplication caused by PLK4. If the stress signals do not cease, p53 becomes active in a later phase of the stress response and through inhibition of PLK4 induces apoptotic death.

In cancer cells, these two proteins (p53 and MKK4) regulating PLK4 activity under stress are often simultaneously inactivated. One can easily imagine the consequences: PLK4 activity persists in the affected cancer cells when they have experienced stress and supernumerary centrosomes arise, leading to chromosome missegregation and, therefore, enhanced tumorigenesis (Nakamura et al. 2013).

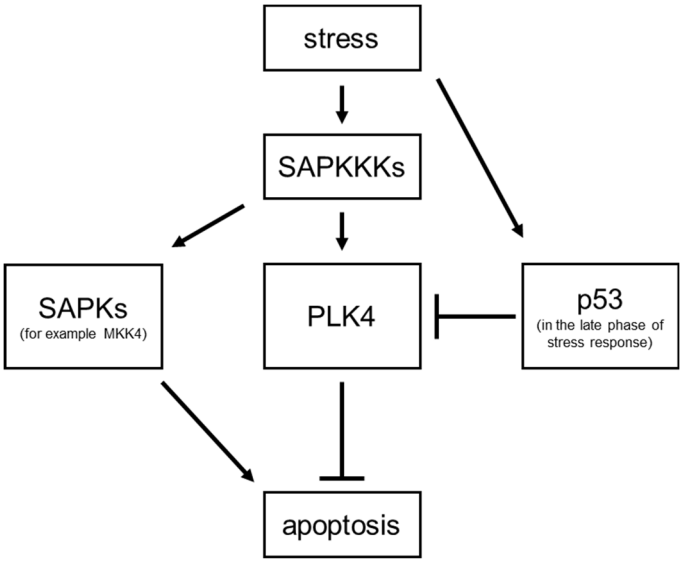

Figure 2: PLK4 regulation in the cellular stress response (as described by Nakamura et al. 2013). When experiencing stress, the SAPK (stress-activated protein kinase) pathway is being activated. This pathway exerts a bimodal function on apoptosis: on the one hand, it activates pro-apoptotic SAPKs, on the other hand, it leads to activation of PLK4, a kinase that acts anti-apoptotic under these circumstances. In healthy cells, this bimodal effect leads to a reciprocal limitation of pro- and anti-apoptotic signals. In the late phase of the physiological stress response, p53 becomes active, inhibiting PLK4 and thereby providing a time-limit for repair mechanisms.

In healthy tissue, PLK4 is a low-abundance enzyme. In many types of cancer, such as lung adenocarcinoma, glioblastoma, gastric cancer and embryonal brain tumors, PLK4 levels have been found upregulated and associated with a worse outcome (Kawakami et al. 2018a; Zhang et al. 2019; Shinmura et al. 2014; Sredni et al. 2017). This renders PLK4 a desirable target for specific cancer therapy.

Recent evidence also assigns to PLK4 a role in regulating cell motility, ultimately linking increased PLK4 activity in cancers to more aggressive behavior with higher risk of cancer progression, invasion and resistance to therapy (Rosario et al. 2015; Kazazian et al. 2017; Tian et al. 2018; Luo et al. 2019).

1.1.3.3 Aurora kinase B (AURKB)

AURKB is a highly conserved protein kinase with several important roles during cell division. It is responsible for the proper attachment of chromosomes to both spindle poles and thus for obtaining a chromosome biorientation (Carmena and Earnshaw 2003).

As part of the spindle assembly checkpoint (SAC), AURKB monitors the correct localization of chromosomes. At this checkpoint, mitosis gets slowed down until all chromosomes display a bipolar orientation. Furthermore, AURKB controls the last steps of cytokinesis, rendering the cell unable to complete cytokinesis when AURKB is not present (Carmena and Earnshaw 2003).

These functions highlight AURKB's importance in cell division. Concordantly, overexpression of AURKB correlates with chromosomal instability and can be found in many non-small cell lung carcinoma (NSCLC) cell lines (Smith et al. 2005).

1.2 Small molecule inhibitors of PLK4

I outlined above some characteristics of PLK4: It has a role in cellular stress response, it is often overexpressed in human malignancies and PLK4 overexpression in tumors contributes to aggressive behavior as well as to resistance to therapy. These characteristics render PLK4 a desirable target for cancer therapies addressing replicative stress pathways (1.1.2). In the following, I am going to describe two inhibitors of PLK4 known today.

1.2.1 Centrinone

Centrinone is a highly selective and reversible inhibitor of PLK4, showing more than 1000-fold selectivity over Aurora kinase A/B in vitro (Wong et al. 2015).

Our group demonstrated before that intact centrosomes are necessary for the proper progression of DNA replication forks (Tayeh et al. 2020). In other words, disruption of the centrosomes leads to replicative stress and to a subsequent DNA damage response. Centrinone disrupts centrosomes by inhibiting PLK4. Thus, treatment with Centrinone leads to replicative stress and a DNA damage response (Tayeh et al. 2020).

According to our previous results, the cascade mediating the DNA damage response in case of PLK4 inhibition is concordant with the signaling pathway explained in 1.1.1: Inhibiting PLK4 disrupts the centrosomes and causes cellular stress. MLK3, a SAPKKK, is activated by stress and in turn activates p38. The kinase p38 then activates the checkpoint kinase MK2, leading to a halt of the cell

cycle at the G2/M transition and to impaired replication fork progression (see **Figure 3**; Tayeh et al. 2020).

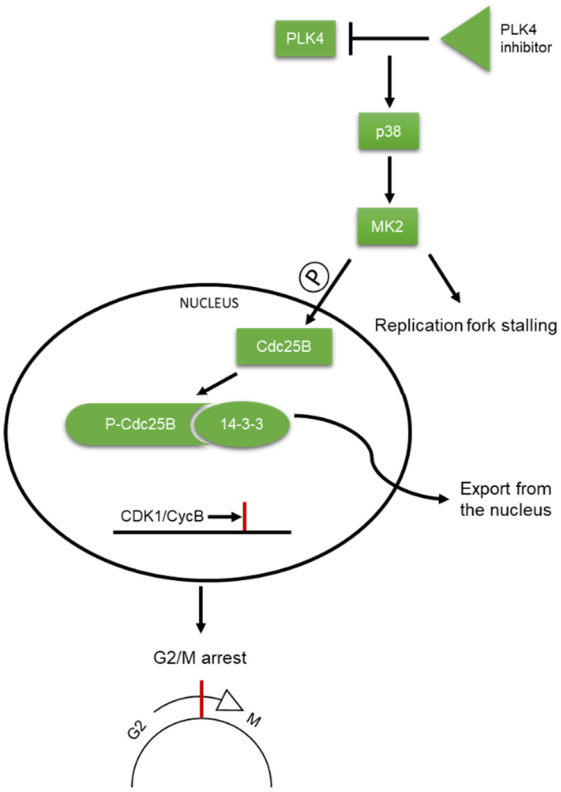

Figure 3: G2/M cell cycle arrest induced by Centrinone. Centrinone selectively inhibits PLK4. This inhibition causes stress in the cell and stress activates MLK3, a SAPKKK (not shown). MLK3 activates p38, p38 activates MK2 (Tayeh et al. 2020). MK2, on the one hand, leads to slower replication fork progression, on the other hand it phosphorylates Cdc25B, a phosphatase that normally activates the CDK1/CyclinB complex which promotes the G2/M transition. Through phosphorylation of Cdc25B by MK2, Cdc25B binds to the 14-3-3 protein and by this is marked for export from the nucleus. CDK1/CyclinB cannot be activated, and the cell is arrested in G2/M (Reinhardt et al. 2010; Thornton and Rincon 2009).

1.2.2 CFI-400945

CFI-400945 (from now on CFI) is an ATP-competitive PLK4 inhibitor. It inhibits PLK4 with an EC_{50} of 12,3 nM. Strikingly, AURKB is also inhibited by CFI at an EC_{50} of 102 nM. Consequently, AURKB might also be affected by CFI at concentrations that sufficiently inhibit PLK4 kinase activity (Mason et al. 2014).

CFI is orally bioavailable and has demonstrated efficacy in various tumor cell lines (Sredni et al. 2017; Kelleher et al. 2018; Kerschner-Morales et al. 2020).

Furthermore, it has been tested in different preclinical mouse tumor models (Mason et al. 2014; Kawakami et al. 2018a; Lohse et al. 2017).

Moreover, in experiments with pancreatic tumor xenografts, CFI managed to increase survival and inhibit tumor growth in most of the models. Within these xenografts, CFI seemed to be most effective against clinically aggressive tumors showing high hypoxia, rapid growth and rapid metastasis. As an advantage towards many other currently available treatments of pancreatic cancer, no drug-resistant cells emerged with CFI (Lohse et al. 2017).

A clinical phase I trial with CFI has been completed for advanced solid tumors, showing preliminary antitumor activity and a favorable tolerability of CFI in these patients (Veitch et al. 2019). Currently, four more clinical trials are being conducted with CFI; one of them in phase I (Relapsed/Refractory AML/MDS; Study Start: 05/2018; ClinicalTrials.gov Identifier: NCT03187288) and three in Phase II: dealing with Prostate Cancer (Study Start: 12/2017; ClinicalTrials.gov Identifier: NCT03385655), Advanced/Metastatic breast cancer (Study Start: 12/2018; ClinicalTrials.gov Identifier NCT03624543) and Advanced Triple Negative Breast Cancer (Study Start: 12/2019; ClinicalTrials.gov Identifier: NCT04176848).

All in all, the effect of CFI in many kinds of tumors has been shown. CFI is said to inhibit cell proliferation, to produce polyploidy and multinucleation. Still, the mechanisms of how the drug achieves these effects remain a matter of ongoing discussion.

1.3 Aim of the thesis

As outlined above, the PLK4 inhibitor Centrinone manages to execute replicative stress on cancer cells by the activation of MLK3 – p38 – MK2.

The aim of my work is to determine whether CFI-400945, another PLK4 inhibitor that is currently in several phase I and II clinical trials, executes replicative stress on cancer cells in the same way as Centrinone. Additionally, a possible drug combination of CFI with MK2 inhibition is examined regarding its impact on DNA replication and cell proliferation.

2 Materials

2.1 Technical devices

Table 1: Technical devices

Device	Supplier
Blotting chamber	Biozym
Cell counting chamber *Neubauer improved*	Brand
Centrifuge *5415R*	Eppendorf
Centrifuge *5810R*	Eppendorf
Chemiluminescence imager *Chemocam HR 16 3200*	Intas Science Imaging Instruments
Cytometer *Celigo*	Cyntellect
Electrophoresis system for SDS-PAGE	Amersham Biosciences
FACS machine *Guava PCA-96 Base*	Millipore, Merck
Freezer -20°C	Liebherr
Freezer -80°C	Heraeus, Thermo Scientific
Heating Block *Thermomixer comfort*	Eppendorf
Incubator for cell culture *Hera Cell 150*	Heraeus, Thermo Scientific
Laminar flow cabinet *Hera safe*	Heraeus, Thermo Scientific
Magnetic stirrer *MR Hei-Standard*	Heidolph
Microscope *Axio Scope.A1*	Zeiss
Mini Centrifuge *MCF-2360*	LMS
pH-meter *WTW-720*	WTW
Pipets Eppendorf Research Series 2100	Eppendorf

Device	Supplier
Power Supply	Biometra
Refrigerator 4°C	Liebherr
Roller *RM5 V-30*	CAT
Scales Acculab *ALC-6100.1*	Sartorius
Sonication device *Bioruptor*	Diagenode
Spectrophotometer *NanoDrop ND-1000*	PeqLab
Thermomixer Comfort	Eppendorf
Vacuum pump	IBS Integra Biosciences
Vortex *Genie 2*	Scientific Industries

2.2 Consumables

Table 2: Consumables

Product	Supplier
Cell culture dishes (10 cm, 15 cm)	Greiner
Cell culture plate 24-well	Costar
Cell culture plates (6-well, 12-well)	Greiner
Cell scraper (16 cm, 25 cm)	Sarstedt
Cellstar Cell Culture Flasks (25 mL)	Greiner
Chamber slides 8-well	Nunc, Thermo Scientific
Coverslips	Menzel
Cryo tubes for cell freezing	Nunc
Glass pipets (5 mL, 10 mL, 25 mL)	Sarstedt
Glass Slides Superfrost	Menzel

Product	Supplier
Pipet tips (10 µL, 20-200 µL, 1,000 µL)	Greiner
Protran nitrocellulose transfer membrane	Whatman
Reaction tube (0.5 mL, 1.5 mL, 2.0 mL)	Eppendorf
Reaction tube (15 mL, 50 mL)	Greiner
Syringe canula	B. Braun
Whatman paper	Whatman

2.3 Chemicals and reagents

Table 3: Chemicals and reagents

Chemical	Supplier
Acetic Acid	Roth
Albumin Fraction V (Bovine Serum Albumin)	Roth
Ammonium persulfate (APS)	Roth
Calcium chloride dehydrate ($CaCl_2$ x $2H_2O$)	Roth
Chlorodeoxyuridine (CldU)	Sigma-Aldrich
Dimethyl sulfoxide (DMSO)	AppliChem
DAPI	Sigma-Aldrich
Ethanol 99.8%	Roth
Fluorescent Mounting Medium	DakoCytomation
Glycerol >99% p.a.	Roth
Glycine >99% p.a.	Roth
Guava ICF Cleaning Solution	Millipore, Merck
Hydrogen chloride/hydrochloric acid (HCl)	Roth
Iododeoxyuridine (IdU)	Sigma-Aldrich
Isopropanol	Roth

Chemical	Supplier
Lipofectamine 3000 (LPF 3000)	Invitrogen
Methanol >99% (MetOH)	Roth
$MgCl_2$ hexahydrate ($MgCl_2$ x $6H_2O$)	Roth
Milk powder	Roth
Nail polish	Essence
PageRuler Prestained Protein Ladder	Fermentas
Paraformaldehyde (PFA) 37%	Sigma-Aldrich
Pefablock SC protease inhibitor	Roth
Pepstatin A	AppliChem
Ponceau S	Roth
Potassium Chloride (KCl)	AppliChem
Potassium dihydrogen phosphate (KH2PO4)	Roth
Propidium iodide (PI)	Sigma-Aldrich
RNAse A	Qiagen
Rotiphorese Gel 30	Roth
Sodium chloride (NaCl)	Roth
Sodium dodecyl sulfate (SDS)	Roth
Sodium ethylene diamine tetra-acetic acid (Na-EDTA)	Roth
Sodium hydroxide (NaOH)	Sigma-Aldrich
Sodium(di-)hydrogenphosphatedihydrate (Na2HPO4) x 2H2O	Roth
Tetramethylethylenediamine (TEMED)	Roth
Thymidine	Sigma-Aldrich
Trisamine (Tris) Pufferan >99% p.a.	Roth
Triton-X100	AppliChem

Chemical	Supplier
Tween 20	AppliChem
Urea	Roth
Vectashield mounting medium	Vector Laboratories

2.4 Buffers and solutions

Table 4: Buffers and solutions

Cell Lysis buffer	
Urea	2 M
Ripa lysis buffer	73.8%
Pefa	1%
PA	0.1%
L/A	0.1%

Western Blot Transfer Buffer	
Tris	25 mM
Glycin	192 mM
MetOH	20%
dissolved in ddH2O (double-distilled water)	

RIPA Lysis Buffer	
Triton-X 100	1%
Na-deoxycholate	1%
SDS	0.1%
NaCl	150 mM
EDTA	10 mM
Tris-HCl pH 7.5	20 mM
Trasylol	100000 KIU
dissolved in ddH2O	

Ponceau S	
Ponceau S	0.5%
Acetic Acid	1%
dissolved in ddH2O	

Fiber Assay Blocking Solution	
BSA (bovine serum albumin)	3%
Tween20	0.1%
in PBS pH 7.4	

6x Laemmli Buffer	
Tris, pH 6.8	0.35 M
Glycerin	30%
SDS	10%
Dithiothreitol	9.3%
Bromophenol blue	0.02%
dissolved in ddH2O	

Phosphate Buffered Saline (PBS)	
NaCl	24 mM
KCl	0.27 mM
Na2HPO4x7H2O	0.81 mM
KH2PO4	0.15 mM
dissolved in ddH2O	

SDS-PAGE Running Buffer	
Tris	25 mM
Glycin	86.1 mM
SDS	3.5 mM
dissolved in ddH2O	

Fiber Assay Spreading Buffer	
Tris, pH 7.4	200 mM
EDTA	50 mM
SDS	0.5%
dissolved in ddH2O	

Western Blot Blocking Solution	
BSA	5%
dissolved in TBS-T	

Fiber Assay Fixative	
MetOH	75%
Acetic Acid	25%

Tris Buffered Saline (TBS) + Tween20 (TBS-T)	
Tris	50 mM
NaCl	150 mM
Tween20	0.1%
dissolved in ddH2O	

IF Blocking Solution	
BSA	3%
dissolved in PBS	

2.5 Commercial kits

2.6 Pharmacological inhibitors

Table 5: Pharmacological inhibitors

Name	Target	Supplier
CDK4 inhibitor	CDK4	Sigma-Aldrich
Centrinone	PLK4	MedChem Express
CFI-400945	PLK4	Cayman Chemicals
MK2 inhibitor III	MK2	Calbiochem

2.7 Oligonucleotides

Table 6: Small interfering RNAs (siRNAs).

All siRNAs are Silencer Select from Ambion, Life Technologies and have stock concentrations of 50 µM.

Name	siRNA ID	Sequence
ctrl#1	neg. control #1	undisclosed
ctrl#2	neg. control #2	undisclosed
MK2#1	s569	sense: 5'- GGAUCAUGCAAUCAACAAAtt -3'
		antisense: 5'- UUUGUUGAUUGCAUGAUCCaa -3'
MK2#2	s570	sense: 5'- CAGUAUCUGCAUUCAAUCAtt -3'
		antisense: 5'- UGAUUGAAUGCAGAUACUGga -3'

2.8 Antibodies

Table 7: Primary antibodies for western blot analysis.

All antibodies were diluted in 5% BSA dissolved in TBS-T.

Target	Supplier	Origin	Dilution	Catalogue nr.
PLK4	Proteintech	rabbit	1:500	1295
Phospho-MK2 (Thr334)	Cell Signalling	rabbit	1:500	3007S
P-Hsp27 (S82)	Cell Signalling	rabbit	1:500	2401L
yH2AX (Ser139)	Millipore	rabbit polyclonal	1:2000	07-164
Hsc70	Santa Cruz	mouse	1:15000	sc-7298

Table 8: Secondary antibodies for western blot analysis.

All antibodies were diluted in 5% BSA dissolved in TBS-T.

Target	Supplier	Dilution	Catalogue nr.
HRP-coupled AffiniPure F(ab')2 fragment, anti-mouse IgG (H+L)	Jackson Immunoresearch	1:2500	711-036-152
HRP-coupled AffiniPure F(ab')2 fragment, anti-rabbit IgG (H+L)	Jackson Immunoresearch	1:2500	715-036-150

Table 9: Primary antibodies for immunofluorescence.

Dilutions were prepared in Fiber Assay Blocking Solution.

Target	Supplier	Origin	Dilution	Catalogue nr.
BrdU/CldU (clone BU1/75)	abcam	rat	1:200	ab6326
BrdU/IdU (clone B44)	Becton Dickinson	mouse	1:200	347580
Anti-Pericentrin	abcam	mouse	1:200	ab28144

Table 10: Secondary antibodies for immunofluorescence (IF).

Dilutions were prepared in Fiber Assay Blocking Solution/IF Blocking Solution (see 2.4 Buffers and solutions) according to the respective experiment.

Target	Supplier	Dilution	Catalogue nr.
Alexa-Fluor-488 goat anti mouse	Invitrogen, Life Technologies	1:150	A-11017
Alexa-Fluor-555 goat anti mouse	Invitrogen, Life Technologies	1:200	A-11003
Alexa-Fluor 594 goat-anti rabbit	Invitrogen, Life Technologies	1:200	A-11012

2.9 Cell culture reagents and media

Table 11: Cell culture reagents and media

Reagent	Supplier
Ciprofloxacin	Bayer
DMEM powder	Gibco, Life Technologies
Fetal Calf Serum (FCS)	Gibco, Life Technologies
L-glutamine	Gibco, Life Technologies
Penicillin/Streptomycin	Gibco, Life Technologies
Trypsin/EDTA	Gibco, Life Technologies

Dulbecco's modified eagle's medium (DMEM)	
DMEM, powder	10.0 g/L
$NaHCO_3$ (Natriumhydrogencarbonat)	3.7 g/L
HEPES	5.96 g/L
dissolved in H_2O	

Dulbecco's modified eagle's medium (DMEM) with supplements	
DMEM	
FCS	10%
Penicillin/Streptomycin (Pen/Strep)	50 U/ml
L-glutamine	200 µM
Ciprofloxacin	10 µg/ml
in ddH2O	

2.10 Software

Table 12: Software

Software	**Supplier**
AxioVision Zen	Zeiss
Celigo Software	Cyntellect
Excel	Microsoft
GraphPad Prism	GraphPad Software
Guava Express Software	Millipore, Merck
Image Lab 5.2.1	BioRad
ImageJ	General Public License
NanoDrop Software	Peqlab
Zen	Zeiss

3 Methods

3.1 Cell cultivation

H1299 cells were cultivated at 37°C and 5% CO_2 in DMEM with supplements. For sub-cultivation, cells were incubated with Trypsin/EDTA at 37°C for 5 minutes, the reaction was stopped with DMEM containing FCS and cells were re-seeded at the desired ratios.

3.2 Transient transfection of cells

200,000 cells per flask were seeded in 25 mL cell culture flasks. Cells were transfected with siRNA (small interfering RNA) using a reverse transfection protocol. A transfection mix using a final concentration of 10 nM siRNA was prepared by first incubating the single components (siRNA, LPF3000) separately in DMEM without supplements (Solution A and B; see **Table 13**). After incubating these solutions for 5 minutes at room temperature, they were combined with each other and incubated for another 20 minutes. Afterwards, this mix along with cells in medium was added to the wells of a cell culture dish. The cells were incubated in the transfection medium for 24 hours at 37 °C and 5% CO_2. After 24 hours, the transfection medium was washed out and replaced by DMEM with supplements. Another 24 hours later, cells were treated according to the respective protocol.

Table 13: Transfection reagents per flask

Solution A	0.5 µL 50 µM siRNA 250 µL DMEM without supplements
Solution B	5 µL LPF3000 250 µL DMEM without supplements

3.3 Chemical treatments

All inhibitors were dissolved in DMSO and aliquoted as instructed by the supplier. Treatments were diluted in pre-warmed medium as shown in **Table 14**. Control samples were obtained by diluting the solvent instead of the inhibitor with medium.

Table 14: Inhibitor concentrations

Name	Target	Solvent	Stock concentration	Working concentration
Centrinone	PLK4	DMSO	10 mM	300 nM/500 nM
CFI-400945	PLK4	DMSO	10 mM	10 nM/50 nM
MK2i III	MK2	DMSO	10 mM	5 µM/10 µM

3.4 Cell synchronization using CDK4 inhibitor and thymidine

In order to examine replicative stress independent of mitosis-related effects, our group developed a protocol for synchronizing cells in G1 for the whole period of treatment. The protocol only allows the cells to enter S phase immediately before harvest. This ensures two requirements: Firstly, to have enough harvested cells in S phase to analyze in the fiber assay. Secondly, and more importantly, to guarantee that these cells have never gone through mitosis throughout their treatment. This ensures that effects like impaired replication fork progression seen in a DNA fiber assay cannot be mediated by mitotic failure but have to be S phase-related.

In order to achieve this, first of all, CDK4 inhibitor (5 µM) was added to cells on a large cell culture dish. After 24 hours (having arrested most of the cells in G1), cells were transfected with siRNA and seeded at a density of 400,000 cells per flask for fiber assay and 200,000 cells per well on six-well dishes for FACS (fluorescence-activated cell sorting) analysis. Again, CDK4 inhibitor was added to the cells. Another eight hours later, cells received additional treatment (PLK4 inhibitor), again coupled with CDK4 inhibitor (see **Figure 4**).

20 hours before the fiber harvest, CDK4 inhibitor was washed out of the cells and thymidine was added (treatments were refreshed, too). Thymidine arrests cells in early S phase, ensuring that cells enter S phase in a more synchronized way than with CDK4 inhibitor alone. Cells were released from the thymidine after 16 hours, enabling them now to enter S phase. FACS samples were retrieved at the time point of release, as well as two and four hours later, to confirm the success of the

synchronization. After four hours, a high proportion of cells was in S phase, and at this point the fiber assay samples were harvested.

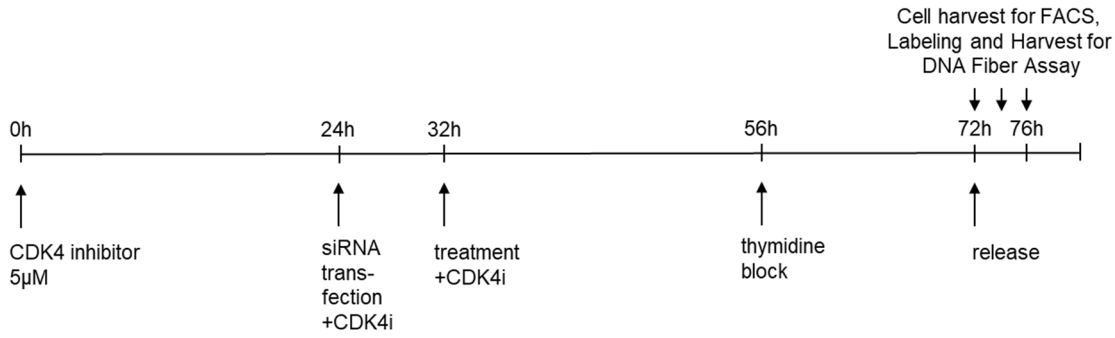

Figure 4: Schematic workflow of cell synchronization using CDK4 inhibitor and thymidine.

3.5 Protein analysis by western blot

In order to analyze changes on a protein level, western blots were performed. Proteins were extracted from the cells with lysis buffer and centrifugation steps, the proteins were separated in size by SDS-PAGE (Sodium dodecyl sulfate polyacrylamide gel electrophoresis) and subsequently, the patterns of protein were transferred (blotted) to a Nitrocellulose membrane. The proteins on the membrane were then detected by specific primary antibodies. Secondary antibodies targeted against the constant region of the primary antibody were added. These secondary antibodies were coupled to horseradish peroxide (HRP). In the end, a solution containing luminol was added. Peroxide oxidates luminol. The amount of light emitted during this reaction is proportional in intensity to the amount of protein and can be captured by a detection machine. This ultimately visualizes the bands of the western blot (Thorpe and Kricka 1986).

3.5.1 Extraction of protein lysates for SDS-PAGE

After treatment, cells were washed twice with ice-cold PBS and detached from the 6-well dishes using cell scrapers. The cells were resuspended in 100-300 µL lysis buffer (see **Table 4**) and sonicated for 10 minutes at high power. All of this protocol was carried out on ice in order to prevent the proteins from degrading. After having sonicated the samples, protein lysates were kept at -80°C until further use.

3.5.2 Bicinchoninic acid (BCA) assay

Relative protein concentrations in the samples were determined using a BCA assay. The solution used for this assay contains bicinchoninic acid and Cu^{2+} ions. When Cu^{2+} ions react with protein, Cu^{1+} ions are generated (Biuret reaction). Cu^{1+} ions form a stable purple complex with bicinchoninic acid. The intensity of the color increases proportionally to the amount of protein available in the sample and can be measured colorimetrically (Smith et al. 1985).

After having determined the concentrations of protein in the samples, all samples were adjusted to the same protein concentration using RIPA buffer. 6x Laemmli buffer was added. Samples were then used for SDS-PAGE or stored at -20°C.

3.5.3 Separation of proteins by SDS-PAGE

SDS-PAGE is a method developed by Shapiro et al. 1967: It separates proteins according to their size. The Laemmli buffer added before the SDS-PAGE contains SDS, an anionic detergent that binds non-specifically to all protein. SDS provides the proteins with a negative electric charge. Thus, when an electric voltage is applied, proteins will migrate towards the anode and separate mainly according to their size and not to their internal charge (Shapiro et al. 1967).

For SDS-PAGE, gels were prepared. First, a resolving gel was poured in between two clean glass plates. To achieve an even surface, it was overlaid with a little amount of isopropanol and left to polymerize for about 45 minutes. Afterwards, the isopropanol was discarded and replaced by a stacking gel. 10-well or 15-well combs were placed in the stacking gel and the gel was left to polymerize again.

This way, a gel with two layers is obtained. These layers differ from each other in their pH and percentages of acrylamide. The pH gradient leads to a concentration of proteins in a tight band: The SDS Running Buffer contains, among others, chloride and glycine ions. At the lower pH of the stacking gel, glycine ions appear as zwitterions. This leads to an entrapment of proteins in between chloride ions (nearer to the anode = leading ions) and glycine ions (further away from the anode = trailing ions) in the stacking gel. When the proteins and ions reach the resolving gel, the pH rises. Glycine loses its zwitterion form and most of it turns into an anion. This way, it passes the proteins and migrates in front of them, concentrating the proteins in a tight band. In the resolving gel, which has smaller

pore sizes due to a higher acrylamide percentage, proteins can separate according to their size: Smaller proteins migrate further than larger proteins which are retained by the pores (Shapiro et al. 1967).

Protein samples with Laemmli buffer were boiled at 95 °C for 5 minutes and loaded into the gel pockets (20-40µL per well), next to a prestained protein ladder for size determination. The electrophoresis was carried out at initially 100V until the resolving gel was reached, then at 120V until sufficient separation.

Table 15: Composition of gels for SDS-PAGE

Ingredients	12% resolving gel	5% stacking gel
H_2O	13.2 mL	13.6 mL
30% acrylamide	16 mL	3.4 mL
Tris	10 mL (1.5 M, pH 8.8)	2.5 mL (1.0 M, pH 6.8)
10% SDS	0.4 mL	0.2 mL
10% APS	0.4 mL	0.2 mL
TEMED	0.03 mL	0.02 mL

3.5.4 Immunoblotting

After separation was achieved, the protein pattern of the gel was transferred to a nitrocellulose membrane. This method called Immunoblotting was first described by Renart et al. (1979) and Towbin et al. (1979). For the transfer, the Nitrocellulose membrane was put on top of the gel. Whatman paper and sponges were added on both sides. Everything was laid into a tank blot chamber filled with ice-cold Western Blot Transfer Buffer (see **Table 4**). In the cold room (4°C), an electric current was applied for 120 minutes at 100V.

3.5.5 Immunostaining

To document the success of the transfer, the membrane was stained with Ponceau S. In case of success, it was blocked with Western Blot Blocking Solution (see **Table 4**) for one hour. Membranes were then incubated with their primary antibodies (in Blocking Solution) at 4 °C over night. The next day,

membranes were washed using TBS-T, blocked three times for 10 minutes with blocking solution and incubated with their secondary antibodies (anti-mouse/anti-rabbit; in Blocking Solution) for one hour. Membranes were washed three times for 10 minutes with TBS-T and developed for western blot using *Immobilon Western HRP Substrate Peroxide Solution* (Millipore) for stronger signals and *SuperSignal West Femto Maximum Sensitivity Substrate* (Femto) for weaker signals.

3.6 DNA fiber assay

DNA fiber assays were performed in order to measure DNA replication speed in a sample. Through this method, impaired replication fork progression can be detected as a determinant of replicative stress (see 1.1.2).

This aim was obtained through consecutive incorporation of two different thymidine analogues into the DNA of sample cells (labeling), their detection by immunostaining and measurement of the resulting fibers' lengths. This way, knowing the amount of replication time that leads to a certain fiber length, the velocity of the DNA polymerases can be deduced.

3.6.1 Labeling

Cells were cultivated in DMEM with supplements in 25 mL flasks at 37 °C. Treatments and siRNA transfections were carried out according to the respective experiment. The day before labeling, stock solutions of the thymidine analogues (CldU and IdU) were boiled at 95 °C for 5 minutes and vortexed well to dissolve everything. They were diluted up to a final concentration of 25 µM (CldU) and 50 µM (IdU) in DMEM with supplements and incubated at 37°C over night.

The day after, the medium with CldU was added to the cells and incubated at 37 °C for 20 minutes. Then it was discarded. The medium with IdU was added to the cells and incubated at 37 °C for 60 minutes. The IdU medium also contained the according treatments of the experiment in order not to release cells from their treatment during labeling time.

3.6.2 Harvest of cells and spreading

Cells were washed twice with ice-cold PBS and harvested in 1-2 mL clean PBS with cell scrapers. Cells were centrifuged at 10,000 rpm and 4 °C for 5 minutes, the supernatant was aspirated, and cells were resuspended in 1 mL clean PBS. 5 µL of the cell suspension were applied to a SuperFrost slide (positively charged) and incubated for 2 minutes. For cell lysis, 10 µL of Fiber Assay Spreading Buffer (see **Table 4**) were carefully mixed with the cells and incubated for another 2 minutes. To spread the cells' content as equally as possible on the slide, the slide was tilted to such an extent that the drop would slowly go to the other end of the slide. The slides were air-dried and afterwards fixed using Fiber Assay Fixative (see **Table 4**) for 10 minutes. Slides were air-dried again and stored at 4 °C for up to several weeks.

3.6.3 Immunostaining

After storage, slides were rehydrated twice for 5 minutes in ddH_2O. They were then equilibrated for 5 minutes in 2.5 M HCl and afterwards denatured in 2.5 M HCl for 80 minutes. Slides were washed twice with PBS (pH 7.4) and incubated twice with Fiber Assay Blocking Solution for 5 minutes each. Then, they were blocked for one hour in Blocking Solution in order to avoid unspecific antibody binding.

Slides were dried and the fibers were incubated with their primary antibodies for one hour. As primary antibodies, two BrdU antibodies (mouse-anti-BrdU and rat-anti-BrdU) were used that are specific for CldU or IdU. Both were diluted in Blocking Solution (1:200), with a total volume of 200 µL per slide.

Afterwards, the slides were washed once with PBS and fixed for 10 minutes with 4% Paraformaldehyde (PFA) in PBS. Again, one washing step with PBS followed. After that, avoiding too much light in order not to lose fluorescence, the fibers were incubated with 150 µL of their secondary antibodies in Blocking Solution (1:200 anti-rat Alexa Fluor 555 and 1:150 anti-mouse Alexa Fluor 488) for at least one and a half hours.

The slides were rinsed twice with PBS and incubated twice with Blocking Solution for 5 minutes each. Again, slides were rinsed once with PBS before mounting with Vectashield mounting medium and sealing with nail polish.

Slides were stored on ice in the dark for a maximum of several days prior to microscope analysis.

3.6.4 Microscopy

Slides were analyzed using an Axio Scope A1 microscope (Zeiss) and filters for 488 nM and 555 nM, an EC Plan-Neofluar 40x objective (Zeiss) and an Axio Cam MRc/503 camera (Zeiss). Five to twenty images per slide were taken using Zen software (Zeiss), and a minimum of two slides per sample were microscoped. To have a representative selection of the cells on the slide, images were taken from different regions of the slide. Fibers were measured and counted using ImageJ. The data was further processed using Microsoft Excel and GraphPad Prism.

3.7 Immunofluorescence

To study the effect of different treatments on centrosomes, an immunofluorescence was performed. Following treatment of cells, centrosomal components were visualized using an anti-Pericentrin antibody with a secondary fluorescent antibody. For staining DNA, and thereby the nucleus, DAPI was used. The number of centrosomes per cell was counted manually and average numbers of centrosomes per cell were determined.

3.7.1 Cell harvest and staining

Cells were cultivated in 8-well chamber slides. For staining and fixation, the medium was removed, and the cells were washed with PBS (carefully in order to avoid cells from being washed away). Cells were then fixed with 4% PFA in PBS for 30 minutes at RT (room temperature). Afterwards, cells were washed twice with PBS and permeabilized with 0.5% Triton X-100 in PBS for 10 minutes at RT. Again, cells were rinsed twice with PBS and blocked for 10 minutes at RT with Blocking Solution (see **Table 4**). Cells were then incubated with 150 µL of their primary antibody (1:200 anti-Pericentrin, abcam) in Blocking Solution for one hour at RT.

Afterwards, cells were rinsed twice with PBS, then incubated with PBS for 5 minutes. 1:500 anti-mouse Alexa Fluor 488 and 1:2000 DAPI were added to 150 µL of Blocking Solution per slide. The cells were incubated with this solution

for 45 minutes at RT in the dark. After repeating the three washing steps from the beginning, the slides were mounted using DAKO mounting medium.

3.7.2 Microscopy

Slides were analyzed using an Axio Scope A1 microscope (Zeiss) and filters for 488 nM and 358 nM, an EC Plan-Neofluar 40x objective (Zeiss) and an Axio Cam MRc/503 camera (Zeiss). 30-45 images per sample were taken, originating from at least two chambers per sample, and processed with Zen (Zeiss). Further analysis was conducted with Zen as well, calculating for each picture the average number of centrosomes per cell and in the end taking all single picture averages together and calculating from them the overall average of centrosomes per cell.

3.8 Flow cytometry

For examining cell cycle distribution, cells were seeded at a density of 100,000 cells per well on 6-well dishes. Following treatment, these cells were harvested, fixed and stained with Propidium Iodide (PI) in order to analyze them in a FACS (fluorescence-activated cell sorting) machine focusing on the DNA content.

3.8.1 Cell harvest and fixation

After the desired treatment period, the medium was aspirated, cells were washed with PBS three times and incubated for 5 minutes at 37 °C with 500 µL trypsin per well. Afterwards, 1 mL warm medium was added per well to stop the trypsinization. Cells were thoroughly resuspended and transferred into 2 mL tubes. After 7 minutes of centrifugation at 2000 rpm and RT, the supernatant was aspirated carefully, and the pellet was resuspended in 1 mL PBS. The centrifugation was repeated and subsequently, the pellet was resuspended in 200 µL cold storage buffer containing 1% FCS in PBS. The suspension was kept on ice and 480 µL 100% ethanol were added in single drops so that a final concentration of 70% ethanol would be obtained. The samples were stored at -20 °C for at least 24 hours and up to two weeks.

3.8.2 Staining

Afterwards, the samples were centrifuged again at 3000 rpm and RT for 7 minutes. The supernatant was removed, and the cells were resuspended in 1 mL PBS for rehydration (10 minutes). Cells were centrifuged again and resuspended in 400 µL PBS with 200 µg/mL RNase A. The suspension was incubated at RT for 30 minutes in order to inactivate DNases within the samples. After this incubation period, 6 µL PI per well was added into the wells of a 96-well plate. 100 µL of the cell suspension was thoroughly resuspended and added to each of the wells. PI and cell suspension were briefly mixed by pipetting and the staining solution was incubated in the dark at RT for about five to 30 minutes.

3.8.3 Analysis

DNA content of the single cells was assessed, and graphs were established using the flow cytometer Guava PCA-96 Base and the Guava Express Software.

3.9 Cell proliferation assay

For the analysis of cell proliferation, cells were seeded at a density of 3,000 cells per well on a 24-well cell culture dish. The cell proliferation was determined through measurement of the cell confluence via an automated optical microscope, the *Celigo* Cytometer. Treatments were refreshed and measurements were taken every second day. For obtaining a graph, confluence was plotted against time using GraphPad Prism. For each sample, five to six technical replica were averaged.

3.10 Statistical analysis

Statistical Analysis was performed using GraphPad Prism (Version 7 and 8). Significances were calculated using an unpaired 2-sided student’s t-test with an assumed level of significance of $\alpha = 0.05$. P values are displayed in the result figures.

4 Results

4.1 CFI reduces cell proliferation by inducing replicative stress through the p38-MK2 signaling pathway

4.1.1 CFI reduces cell proliferation

In order to find out about the cytotoxic effect that CFI has on cells, a cell proliferation assay was conducted. H1299 cells were seeded on 24-well plates at a density of 3,000 cells per well and treated either with 10 nM CFI or with DMSO as a control. The confluence of the cells was determined using a *Celigo* Cytometer (measurements and refreshment of treatments every second day starting on day zero).

As shown in **Figure 5**, during the first two days of the experiment, the proliferation of CFI-treated cells and of control cells did not differ significantly from each other. Starting from day four, a reduction in the proliferation of CFI-treated cells compared to the control cells can be observed. The confluence of DMSO-treated cells reached 100% on day six whereas CFI-treated cells were only about 65% confluent on the same day. The experiment was conducted another time with comparable results. Surprisingly, in the second trial, the effect was even bigger, leaving CFI-treated cells only at about 30% on day six with the DMSO-treated cells being again 100% confluent on day six. This could be explained by different passage numbers of cells in the two experiments. In any case, the tendency is the same: CFI-treated cells show reduced cell proliferation compared to control cells.

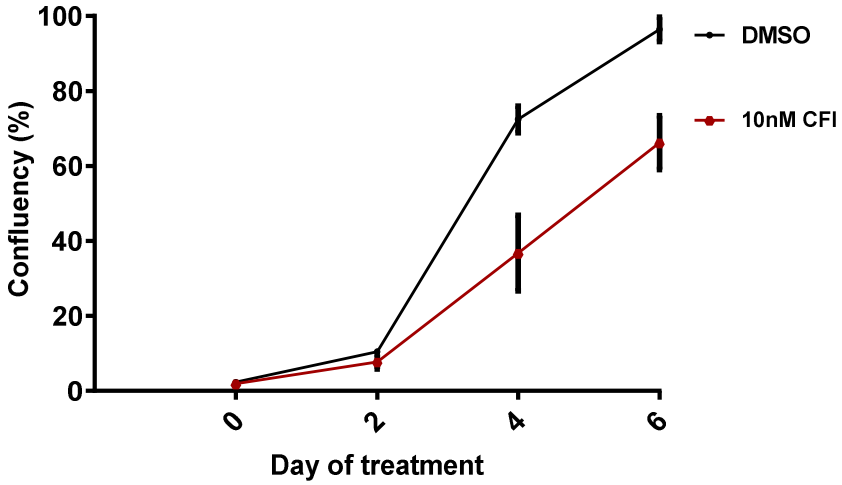

Figure 5: Reduction of cell proliferation by CFI treatment. H1299 cells were treated with 10nM CFI for the indicated amount of time. The first measurement took place on day zero, which was also the first day of treatment. Results were obtained by analysis through a Celigo Cytometer.

4.1.2 CFI impairs the progression of the replication fork

After having shown that CFI treatment leads to reduced proliferation of H1299 cells, we wanted to examine whether this impairment of cell growth results from replicative stress (as it is the case for Centrinone; Tayeh et al. 2020). Therefore, a DNA fiber assay was conducted after 48 hours treatment with CFI (10 nM) or DMSO (control).

Analysis of the fibers showed a significant decrease in fork progression in CFI-treated cells compared to control cells (**Figure 6**). While the control cells showed an average fork progression of about 1 kb/min, CFI-treated cells had an average fork progression of about 0.7 kb/min. The following conclusion can be drawn: replicative stress – which is a consequence of impaired fork progression – might play a role in disturbing cell proliferation in CFI-treated cells.

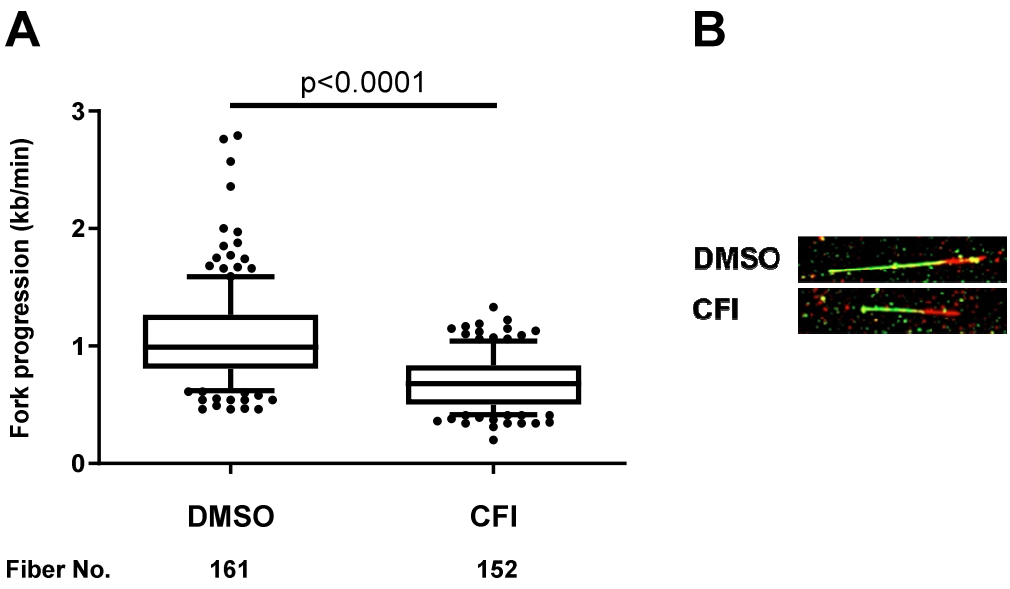

Figure 6: CFI treatment slows down the progression of the replication fork. H1299 cells were treated with CFI (10 nM) for 48 hours. A DNA fiber assay was performed, showing a significant reduction in fork progression after CFI treatment. **A:** Result of the quantification. **B:** Two representative images of fibers.

4.1.3 CFI induces replicative stress through activation of the p38-MK2 signaling pathway

Having shown that replicative stress plays a role in CFI-treated cells, the next aim was to determine the signaling pathways mediating the replicative stress response. One option was the activation of the p38-MK2 signaling pathway (since this is the way the highly-selective PLK4 inhibitor Centrinone exerts replicative stress on cancer cells, Tayeh et al. 2020, see 1.2.1). Thus, a western blot was performed, staining for phosphorylated substrates of kinases of the cascade (P-p38, P-MK2, P-Hsp27), and for yH2AX as another marker for replicative stress.

H1299 cells were treated with CFI (10 nM) or DMSO (control) for 48 hours. A protein analysis was performed (see 3.5). As can be seen in **Figure 7A**, levels of P-p38, P-MK2 and P-Hsp27 were elevated following CFI treatment, indicating that this pathway has been activated. Moreover, yH2AX levels were elevated upon CFI treatment, another proof for the finding that CFI causes replicative stress. It can be concluded that the CFI-induced replicative stress response is mediated by p38-MK2 signaling.

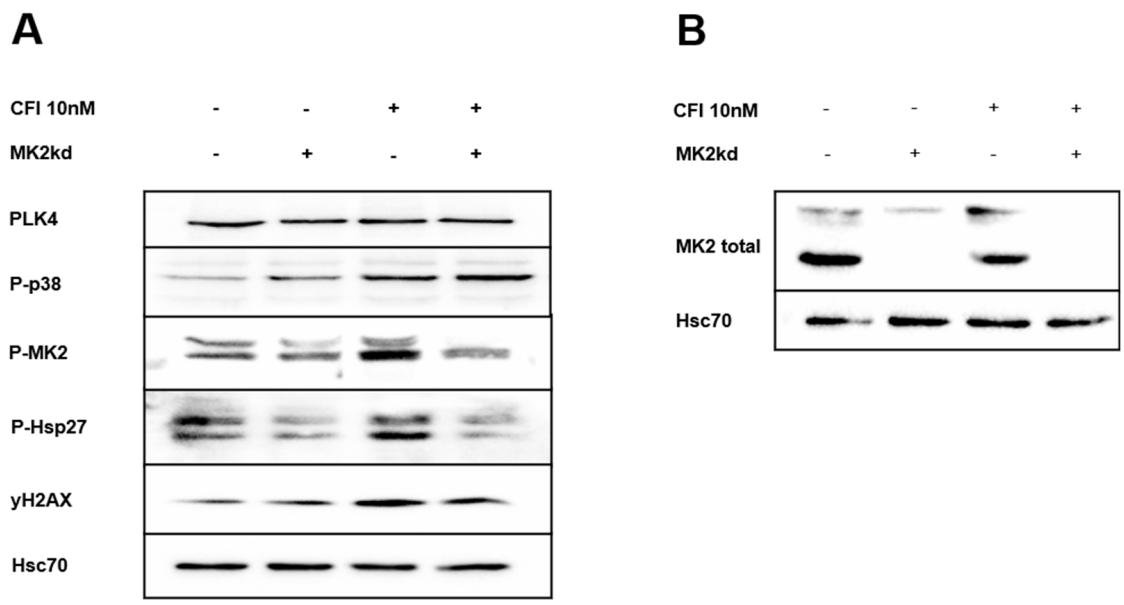

Figure 7: Following CFI treatment, replicative stress is mediated through the p38-MK2 pathway in H1299 cells. A western blot was performed after 48 hours of treatment with either CFI (10 nM) or DMSO (control). **A:** Treatment with CFI leads to activation of p38, MK2, Hsp27 and yH2AX. **B:** Confirmation that the knockdown of MK2 worked.

4.2 Additional MK2 inhibition rescues fork progression but, surprisingly, disturbs cell proliferation to an even greater extent

Having unraveled the p38-MK2 pathway as being activated under CFI treatment, it was of interest whether additional MK2 inhibition or MK2 knockdown could rescue the fork progression. This experiment was necessary in order to confirm the finding of 4.1.3, that the p38-MK2 pathway is responsible for the induction of replicative stress. It was conceivable since the same was the case with Centrinone (**Figure 8C**).

A DNA fiber assay was performed following a 72 hours knockdown of MK2 and a concurrent 48 hours treatment with CFI (10 nM) or DMSO (control). A western blot was performed in order to confirm the successful MK2 knockdown

Figure 7B). As can be seen in **Figure 8A**, the impaired replication fork progression induced by CFI could nicely be rescued by MK2 knockdown. This indicates that the p38-MK2 pathway is responsible for replicative stress caused by CFI.

Additionally, a determination of cell proliferation was performed using the *Celigo* Cytometer. H1299 cells were treated with CFI (10 nM) with and without MK2 inhibitor (10 µM) for a total of six days. Treatments were refreshed and measurements were conducted every second day. Surprisingly, in this cell proliferation assay, the reduction of cell proliferation caused by CFI could not be rescued by additional MK2 inhibition. Quite the contrary, cell proliferation was even further reduced when MK2 inhibition was added. In conjunction with the successful rescue in the fiber assay experiment, these findings indicate two results. MK2 inhibition does prevent replicative stress caused by CFI treatment but replicative stress does not seem to be the only player in decreasing cell proliferation in CFI-treated cells.

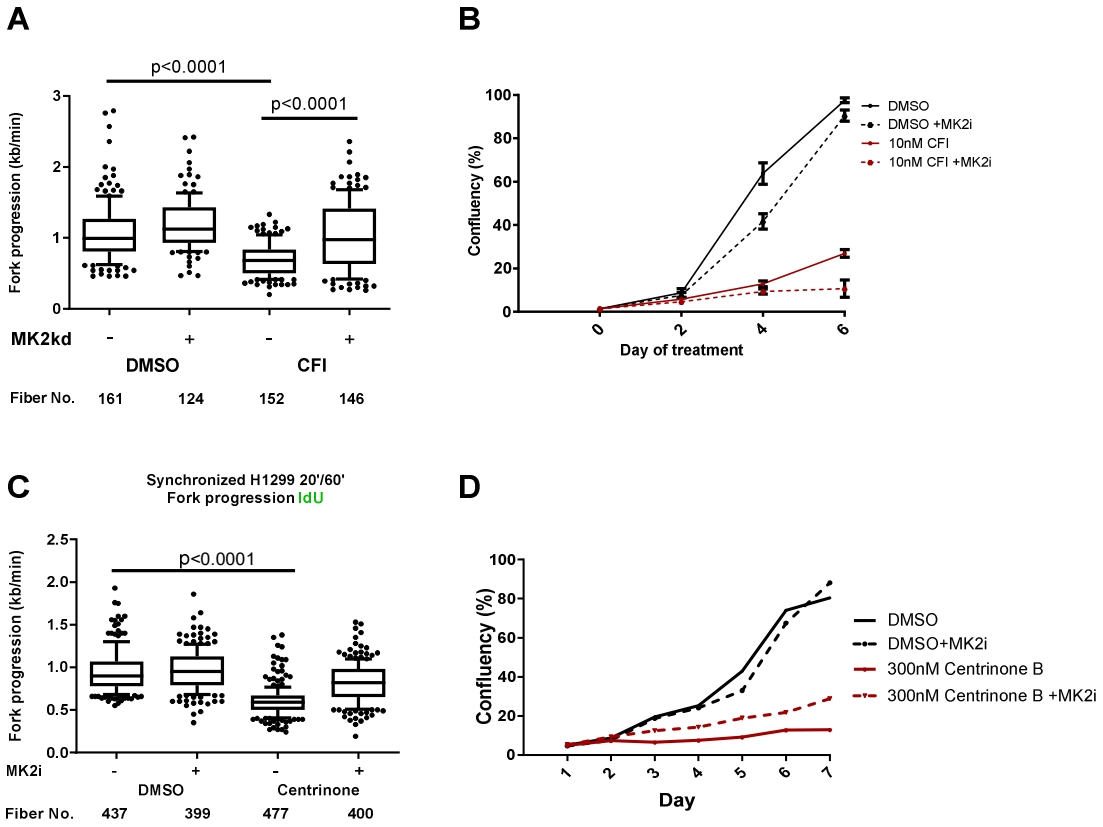

Figure 8: MK2 inhibition upon CFI treatment rescues replication fork progression but increases the reduction of cell proliferation caused by CFI. A: An siRNA-mediated MK2 knockdown in H1299 cells was performed (72 hours), followed by treatment with CFI (10 nM, 48 hours). A DNA fiber assay was performed. **B:** A cell proliferation assay was conducted, examining the combined effects of 10 nM CFI and 10 µM MK2 inhibitor on H1299 cells. **C and D:** The same experiments as in A and B were conducted with 300 nM Centrinone instead of CFI. Experiments in C and D were carried out by *Zainab Tayeh*.

4.3 Centrosome amplification takes place in CFI-treated cells but not in Centrinone-treated cells

Regarding the different reactions towards additional MK2 inhibition upon CFI or Centrinone treatment, it was questionable what the reason behind this might be. In literature, differences on a centrosomal level are discussed: While Centrinone depletes centrosomes, CFI rather duplicates them (Oegema et al. 2018).

To examine this hypothesis, immunofluorescence was performed, co-staining for nuclear (DAPI) and centrosomal material (Pericentrin, PCNT). From the merged pictures the average numbers of centrosomes per cell were determined for Centrinone (500 nM), CFI (10 nM, 50 nM) and DMSO (control).

While for Centrinone, the number of centrosomes per cell was smaller than with DMSO (ca. 0.5 compared to 1 per cell), for CFI the centrosomes increased in number with rising concentrations of CFI. At 10 nM CFI, we saw some cells with supernumerary centrosomes (mean of around 1.4), while at 50 nM, there were many cells with dramatically increased numbers of centrosomes per cell (average of 3.8 with up to 17 centrosomes per cell). This suggests that the number of centrosomes might play a role in the differential response to MK2 inhibition upon Centrinone or CFI treatment.

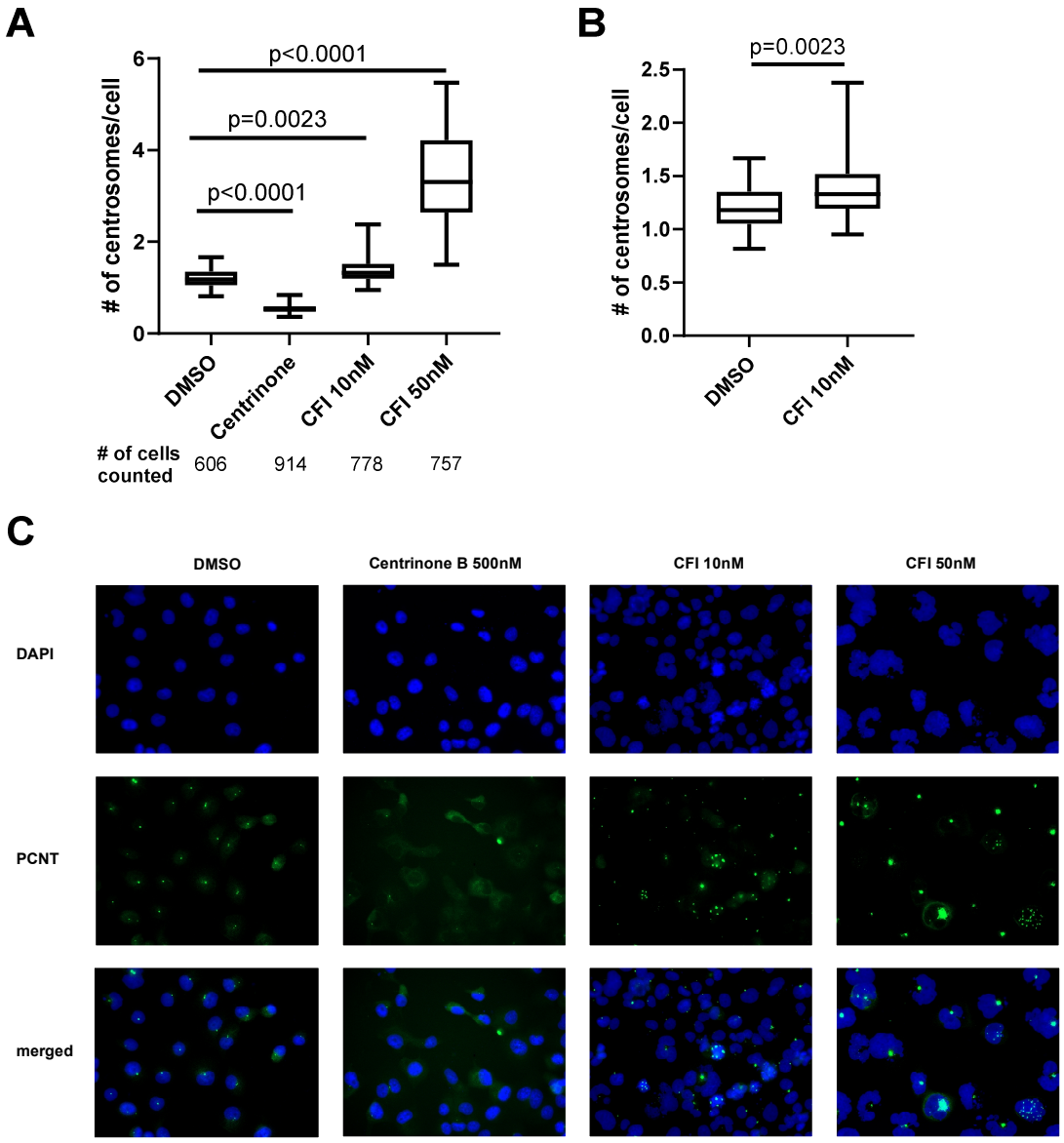

Figure 9: Amplification of centrosomes through CFI treatment. H1299 cells were treated with Centrinone (500 nM), CFI (10 nM, 50 nM) or DMSO (control) for 48 hours. Nuclear content was stained using DAPI, centrosomal material was stained with an antibody to Pericentrin (PCNT). The number of centrosomes per cell was quantified manually. **A:** Quantification results. **B:** Quantification results focusing on 10 nM CFI. **C:** Representative sections from the immunofluorescence images.

4.4 CFI-treated cells become multinuclear and polyploid

As the number of centrosomes was upregulated in CFI-treated cells, it was nearby to hypothesize that CFI treatment would lead to increased mitotic failure. In order to assess the mitotic function after CFI treatment, starting on a very basal level, CFI-treated cells were subjected to light microscopy over a certain time course. H1299 cells were treated with either 10 nM CFI or DMSO for three to five days. Pictures were taken every second day.

As can be seen in **Figure 10A**, the DMSO-treated cells amplified in their number only, while their size stayed roughly the same. On day five, DMSO-treated cells were highly confluent. Meanwhile, CFI-treated cells not only amplified in number but also increased in size, with a mean diameter of about 20-30 µM on day zero to diameters of up to several hundred µM on day five. Furthermore, signs of apoptosis could be seen in CFI-treated cells, becoming more with proceeding time. As indicated by the green arrows, multinucleation of some of the CFI-treated cells became visible. Thus, the increase in size of these cells might be explained by aberrant mitoses.

To support this hypothesis, a flow cytometry analysis of the DNA content of CFI-treated cells (10 nM, 50 nM, **Figure 10B**) was carried out. It became apparent that the amount of polyploid (4N/16N/32N) cells increased with rising concentrations of CFI. This supported the idea that CFI-treated cells had gone through failed mitosis, resulting in maldivision of cells and accumulation of DNA content.

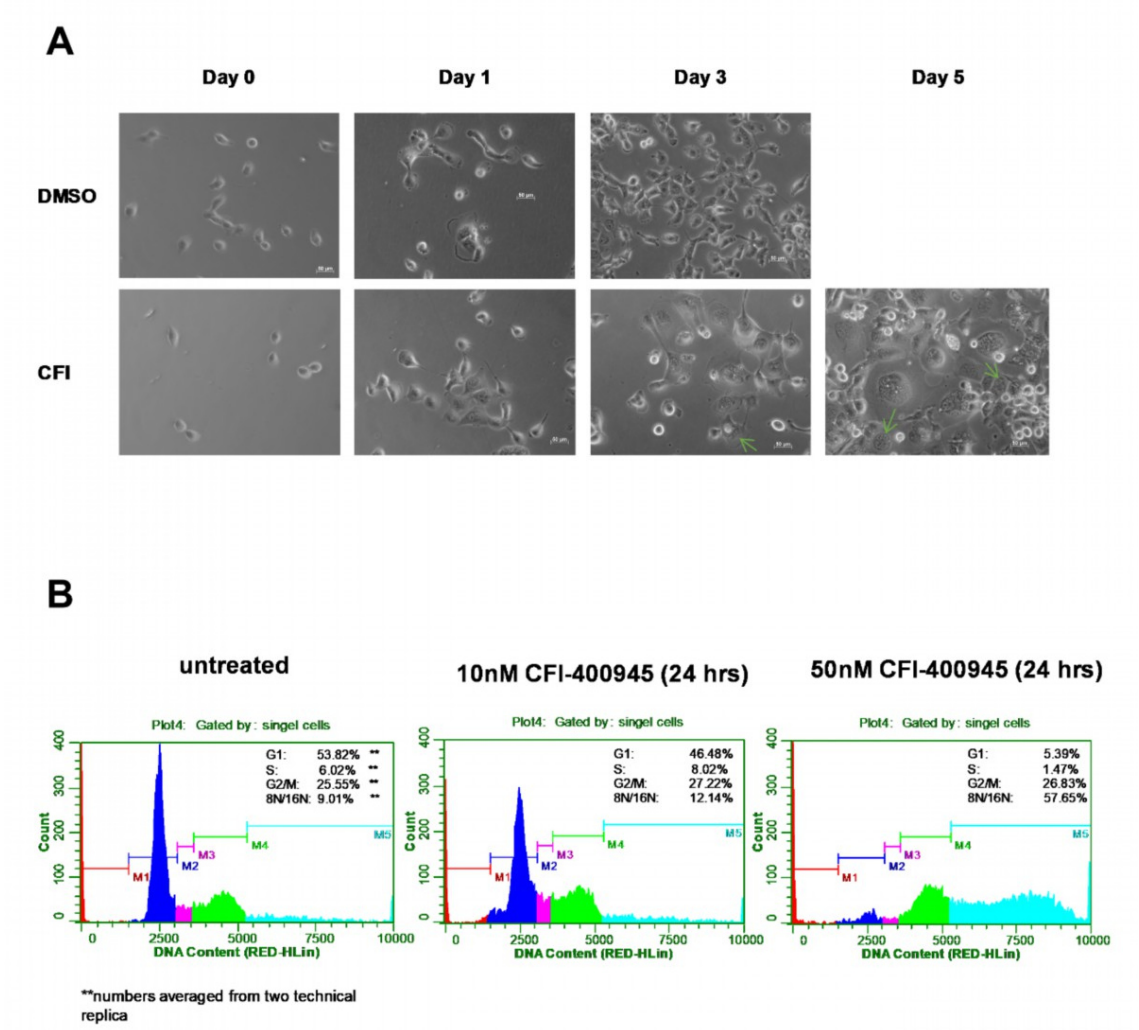

Figure 10: Treatment with CFI leads to formation of multinucleated and polyploid cells. A: H1299 cells were treated with 10 nM CFI or DMSO (control) for the indicated period of time. Light microscopy images were taken in order to document changes in cell morphology. **B:** H1299 cells were treated with different concentrations of CFI for 24 hours. The DNA content of the cells was assessed by flow cytometry.

4.5 CFI induces replicative stress independent of mitosis

Mitotic failure is well-known in the literature to cause replicative stress (Passerini et al. 2016). Having demonstrated that mitotic failure occurs after CFI treatment, it would be tempting to conclude that replicative stress in cells treated with CFI (**Figure 6**) would indirectly be caused by mitotic failure. Alternatively, a direct effect on replication could be imagined. Therefore another fiber assay, this time

using synchronized H1299 cells, was performed. The synchronization workflow is depicted in **Figure 11C** (and described in more detail in section 3.4).

In order to exclude mitotic failure as the reason for replicative stress in CFI-treated cells, it was necessary to make sure that these cells would not pass M phase during their treatment. To achieve this, cells were synchronized in G1 phase using a CDK4 inhibitor. During this arrest, cells were treated with CFI (10 nM) and transfected with siRNA against MK2. 20 hours before harvesting for the fiber assay, a thymidine block was performed, releasing cells only to early S phase. 16 hours after that, cells were released from the thymidine and allowed to proceed further into S phase. The cells were harvested about four hours after the release. **Figure 11B** shows a flow cytometry analysis of the cells at different time points of the synchronization to prove that the synchronization worked out.

As can be seen in **Figure 11A**, the experiment with synchronized cells showed the same tendency as the experiment with asynchronous cells (**Figure 8A**), depicting a decrease of the replication fork progression under CFI treatment and a rescue of this decrease with additional MK2 knockdown. Therefore, even though there is mitotic failure in CFI-treated cells, the mitotic failure seems not to be the main reason for replicative stress.

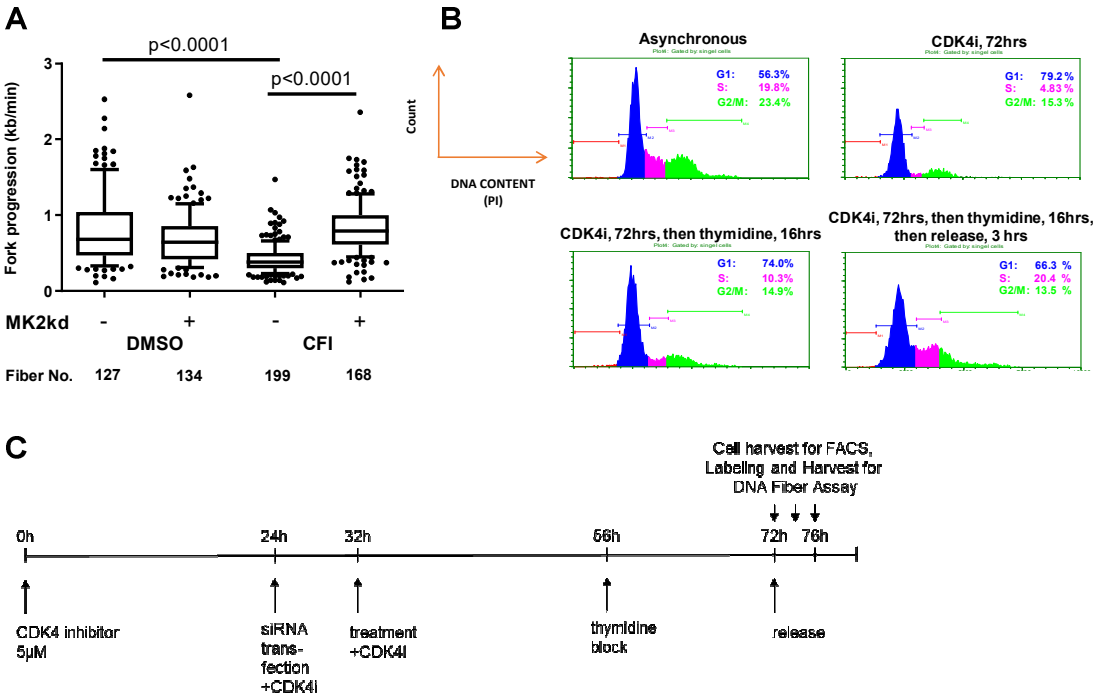

Figure 11: Replicative stress in CFI-treated cells is not solely caused by mitotic failure. A fiber assay was conducted with synchronized H1299 cells. Cells were not allowed to pass mitosis for the time of treatment. **A:** The pattern of replicative stress response of synchronous cells is similar to that of asynchronous cells. **B:** The flow cytometry analysis confirms that the synchronization worked. **C:** Schematic workflow of the synchronization.

5 Discussion

This thesis aimed to understand more about the way the PLK4 inhibitor CFI exerts its cytotoxic effect on cells and whether replicative stress plays a role in it. As CFI is being examined in different phase I and II clinical trials, it is essential to know more about its mechanism of action. Based on that, the impact of CFI on different tumors could be predicted and CFI-sensitive tumors might be selected as promising study models. Furthermore, sound understanding of a drug's mechanisms of action might lead to other treatment approaches, including novel drug combinations.

5.1 Summary of results

We found out that CFI leads to decreased proliferation of H1299 cells. This process is, at least in part, mediated by a decrease in replication fork progression and by replicative stress. The decrease in replication fork progression is achieved by the activation of a pathway including p38 and MK2. The exertion of replicative stress is independent of mitotic failure.

MK2 inhibition may rescue the progression of replication forks but cannot rescue the reduced cell proliferation. Strikingly, cells treated with CFI in combination with an MK2 inhibitor even show less cell proliferation than cells that were only treated with CFI (this experiment was also repeated with the same results by *Zainab Tayeh*). This strongly suggests an additional mechanism besides replicative stress through which CFI reduces cell proliferation.

CFI causes polyploidy and centrosomal amplification – opposing the results of PLK4 inhibition using Centrinone. Upon Centrinone treatment, centrosomes are not amplificated but depleted and cells are rather arrested in G2 instead of becoming polyploid (the FACS experiment with Centrinone was conducted by *Zainab Tayeh*[1]).

These findings illuminate a difference in the mechanisms of action of Centrinone and CFI.

[1] Tayeh Z.: Centrosome integrity as a determinant of replication stress. Molecular Medicine Diss. Göttingen 2019

5.2 Two PLK4 inhibitors act differentially in response to additional MK2 inhibition – off-target effects as a possible reason

Centrinone is a highly selective PLK4 inhibitor. Its effects are recapitulated by PLK4 knockdown. When H1299 cells are transfected with PLK4 siRNA, centrosomes are depleted and cells get arrested in G2/M (experiments conducted by *Zainab Tayeh*). These effects strongly resemble Centrinone treatment which is a striking evidence that Centrinone does inhibit PLK4 only, without off-target effects.

Using CFI, obverse results can be depicted. The observed effects (amplification of centrosomes, polyploidy) do not match the results of PLK4 knockdown. In literature it is discussed controversially whether CFI exhibits an off-target effect against AURKB (Mason et al. 2014; Oegema et al. 2018; Kawakami et al. 2018a, 2018b; Press et al. 2019; Suri et al. 2019). In the following, I am going to explain why we find this off-target effect conceivable, first mechanistically, then by comparison to literature and finally by further experiments.

5.2.1 CFI exerting an off-target effect against AURKB – the mechanistic view

Focusing further on the differences between Centrinone- and CFI-treated cells, one key feature becomes apparent: In contrast to Centrinone, CFI causes polyploidy and multinucleation, conditions that are strongly linked to mitotic failure and mitotic catastrophe (Castedo et al. 2004; Su et al. 2018).

According to Castedo et al. (2004), mitotic failure occurs when DNA damage leads to chromosomal missegregation and functioning cell cycle checkpoints are absent. Mitotic failure results in endoreduplication with tetraploidy after one cell division and polyploidy after several cell cycles. Mitotic catastrophe is the cell's way to escape mitotic failure: Chromosomal missegregation leads to apoptotic death.

How do mitotic failure and mitotic catastrophe take place in our models? As outlined above, two prerequisites are needed: DNA damage and defective cell cycle checkpoints. DNA damage is already present endogenously in cancer cells

and the additional PLK4 inhibition causes even more replicative stress. Defective cell cycle checkpoints can be found in both of our models (Centrinone- and CFI-treated cells): H1299 cells are by nature p53 mutant cell lines. With wildtype p53 controlling the G1/S checkpoint, p53 defective cells can only rely on the G2/M checkpoint (Kawabe 2004).

So far, both of our models show comparable DNA damage and defective cell cycle checkpoints. It would be conceivable that they both undergo mitotic failure and mitotic catastrophe. So what is the difference? This is where we come back to AURKB.

AURKB is important for cell division, especially for the spindle assembly checkpoint (SAC). At the SAC, the correct orientation of chromosomes for the division of sister chromatids is being monitored. If chromosomes are not properly attached to both spindle poles, AURKB slows down mitosis until all chromosomes are correctly orientated (Carmena und Earnshaw 2003).

If AURKB is inhibited, the SAC is abolished, in addition to the abolishment of the G1/S checkpoint in our models. In literature, it is known that AURKB inhibition enhances mitotic catastrophe (Tao et al. 2009; Su et al. 2018;). With the mitotic catastrophe seen in CFI-treated cells but not in Centrinone-treated cells, it is thus conceivable that CFI causes an additional AURKB inhibition.

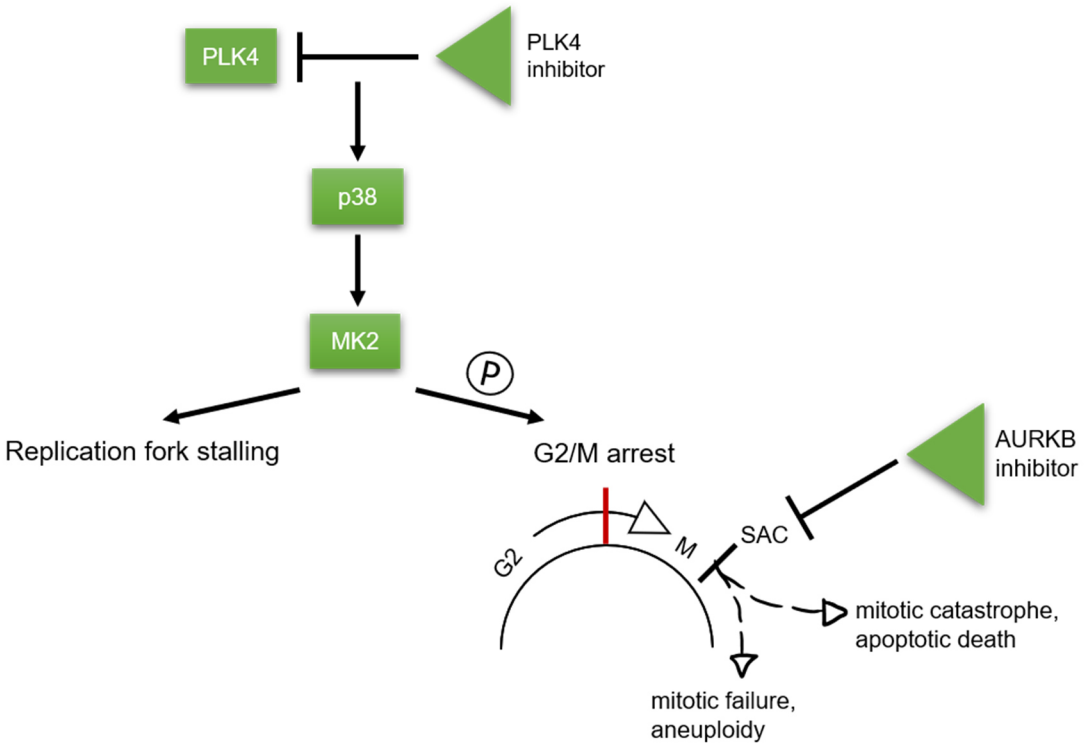

Figure 12: Mechanism of action through which CFI might perform its cytotoxic activity. CFI not only leads to replication fork stalling through PLK4 inhibition but also to mitotic failure and catastrophe through AURKB inhibition.

When it comes to combined Centrinone/CFI and MK2 inhibitor treatment, the G2/M checkpoint is being abolished as well. Centrinone-treated cells can rely on their SAC to sort out cells with severely damaged DNA, thus MK2 inhibition is able to rescue impaired cell proliferation in these cells. CFI-treated cells cannot rely on their SAC and continue their cell cycle with severely damaged DNA. This might be what tips the scales and renders combined CFI and MK2 inhibitor treatment an even more toxic combination against cancer cells than CFI alone (**Figure 12**, **Figure 13**).

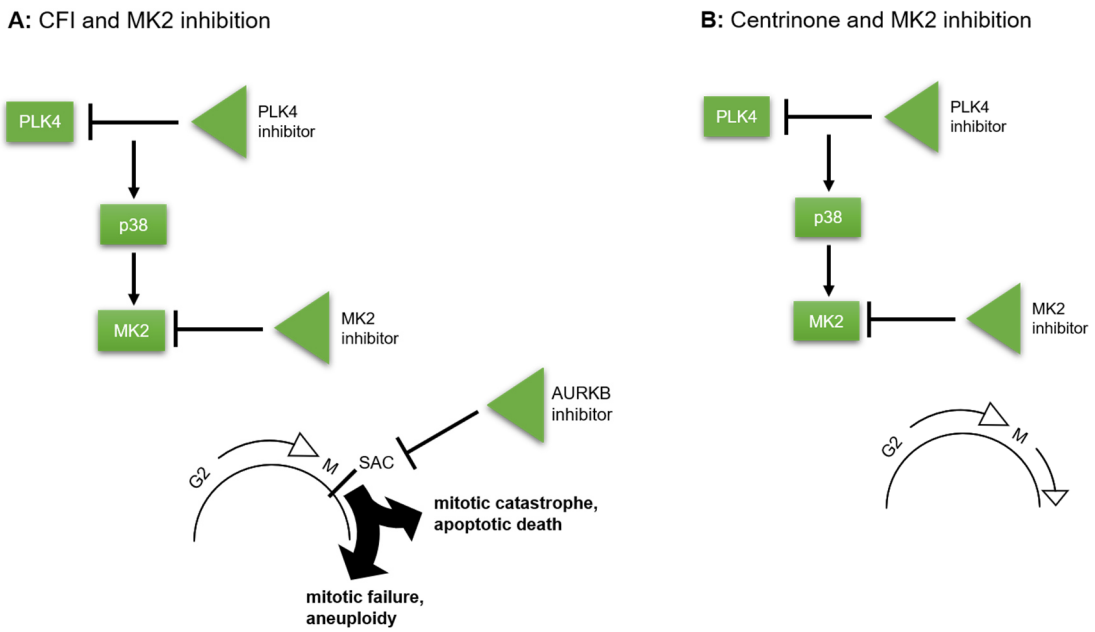

Figure 13: Hypothesized effects of CFI or Centrinone treatment combined with MK2 inhibition. A: MK2 inhibition impairs the G2/M checkpoint. The additional inhibition of AURKB by CFI leads to abolishment of the SAC. Massive mitotic failure and mitotic catastrophe ensue. **B:** In case of Centrinone treatment, MK2 inhibition is able to rescue the effects of PLK4 inhibition (G2/M cell cycle arrest) and the cell cycle continues properly.

5.2.2 An off-target effect of CFI in the literature

Literature mainly supports the theory of CFI exerting an off-target effect against AURKB but doubts remain.

The first article ever published on the cellular effects of CFI examined possible off-target effects in (partly engineered) HCT116 cells. They found significant activity against four kinases: TRKA, TRKB, Tie2/TEK and AURKB. Whilst TRKA, TRKB and Tie2/TEK play a minor role in lung cancer tissue, AURKB can be found in all proliferating cells and plays an important role in cell division (Mason et al. 2014).

Mason et al. also examined centriole numbers in CFI-treated cells and found a bimodal effect: At lower concentrations (10-100 nM), CFI led to an increase in the number of centrioles per spindle pole, at higher concentrations (<200 nM), the number of centrioles per spindle pole was decreased. They explain this finding with partial versus full inhibition of PLK4. PLK4 auto-phosphorylates itself as a

mark for proteasomal degradation, thereby limiting its own effect (i.e. centriole biogenesis). Mason et al. propose that CFI, at lower concentrations, inhibits the auto-phosphorylation of PLK4 only, whereas the ability of PLK4 to phosphorylate effector molecules (leading to centriole biogenesis) remains. Thus, PLK4 is not degraded, it accumulates and causes an effect similar to PLK4 overexpression: centriole numbers increase. However, at higher concentrations of CFI, all PLK4 activity is being inhibited and centriole numbers decrease.

While the centrioles displayed such a bimodal effect, centrosome numbers reacted differently to CFI treatment in the experiments by Mason et al. (2014). With all inhibitory concentrations of CFI, they observed multipolar spindles and increased centrosome numbers per cell. These are effects Mason et al. trace back to a failure to complete cytokinesis, a failure that could likely be caused by AURKB inhibition (see 1.1.3.3).

Kawakami et al. think differently about the off-target effects of CFI. They transferred the experiments on CFI to different lung cancer cell lines. When examining centrosome numbers and cytokinesis, they found the same effects as Mason et al. but assess them differently: At all inhibitory concentrations of CFI, multipolar spindles formed and centrosome numbers increased. In particular, this effect was bigger at low concentrations of CFI and smaller at higher concentrations. Kawakami et al. name this a “bimodal effect” and trace it back to the partial versus full inhibition of PLK4 that Mason et al. describe for centriole numbers. Kawakami et al. thus deny a significant off-target effect of CFI on AURKB.

Oegema et al. (2018) replied to this article with a set of experiments where they compared CFI to Centrinone. They state that CFI causes extensive multinucleation. Centrinone, as a very selective PLK4 inhibitor, does not cause such multinucleation at concentrations depleting most of the centrosomes. Thus, Oegema et al. argue that this multinucleation may not be explained by PLK4 inhibition only. On the contrary, AURKB inhibition would explain the multinucleation in a better way (see 1.1.3.3).

Concerning the centrosomal amplification, Oegema et al. link the two papers by Mason et al. and by Kawakami et al.: They propose that the combined work of AURKB inhibition and partial PLK4 inhibition is responsible for the effects.

Summing up, regarding the partial versus full PLK4 inhibition, it needs to be clearly stated which part of the cell is being addressed. For centrioles, a clear bimodal effect is conceivable: reduction of centrioles per spindle pole at higher concentrations of CFI versus amplification of centrioles at lower concentrations of CFI (Mason et al. 2014).

Other than that, centrosomal amplification takes place at all inhibitory concentrations of CFI. Although at higher concentrations of CFI the effect is not as big as with lower concentrations of CFI, it is still an effect of centrosomal amplification, not one of centrosomal reduction (Oegema et al. 2018). If partial versus full PLK4 inhibition was fully responsible for the reaction of centrosomes to CFI treatment, one would expect that – like for the centrioles – centrosome numbers would increase with lower concentrations of CFI and decrease with higher concentrations of CFI. Unlike that, centrosome numbers do increase in both cases – but to a different extent. This provides a hint that PLK4 inhibition may not be fully responsible for CFI's effects. Partial vs full PLK4 inhibition may well cause the different extent to which centrosomes duplicate, but the underlying effect of centrosomal amplification should rather be caused by a failure of cytokinesis obtained through AURKB inhibition.

5.2.3 Experimental evidence for an off-target effect by CFI

To prove the involvement of AURKB inhibition in CFI's effects, further experiments were conducted by our group. *Kim Stegmann* treated several cells with Centrinone combined with an AURKB inhibitor. This drug combination indeed mimicked the effect of CFI regarding cell proliferation, replication fork speed, nucleus morphology, chromosome number and amount of polyploidy. This further suggests that the difference between CFI and Centrinone is caused by an additional AURKB inhibition carried out by CFI (Stegmann 2019)[2].

[2] Stegmann KM: Combined inhibition of protein kinases to interfere with centrosome integrity and mitosis of cancer cells. Molecular Medicine Master's thesis Göttingen 2019

5.3 Proposing a novel drug synergism

In our experiments, we observed a synergistic effect of CFI and MK2 inhibitor reducing the proliferation of cells. This effect is most probably based on a combined PLK4 and AURKB inhibition by CFI. It mechanistically makes sense (5.2.1) and is supported by literature (Oegema et al. 2018; Mason et al. 2014; Suri et al. 2019) as well as by further experiments (5.2.3). This provides evidence for giving CFI and MK2 inhibitor a try as a drug combination, enhancing mitotic catastrophe by provoking replicative stress and abolishing cell cycle checkpoints.

Moreover, it corresponds to Tao et al. (2009): They suggest that DNA damage combined with a deregulation of the SAC (leading to mitotic catastrophe) could be a general strategy to push cancer cells into death.

5.3.1 A similar drug synergism in the literature

The drug synergism explained above shows similarities to another drug synergism proposed by Kawakami et al. (2018a): They introduced the idea of combining CFI with a CDK2 inhibitor. CDK2 is essential at the G1/S checkpoint. If CDK2 is inhibited, the G1/S checkpoint is abolished. Importantly, cells treated with CFI and CDK2 inhibitor are not deprived of their G2/M checkpoint and can still rely on it.

Regarding the G1/S checkpoints, an advantage of CFI and MK2 inhibitor in p53 mutant cell lines might be predicted. G1/S checkpoints are often endogenously defective in p53 mutant cell lines (for example in H1299 cells). Thus, it might be possible that in these cell lines, the combination of CFI and MK2 inhibitor would be more sufficient than combining CFI with a CDK2 inhibitor.

5.3.2 Possible resistance towards therapy

Using a drug targeting cell cycle checkpoints, caution needs to be taken: Abolishing checkpoints is a double-edged sword. There might always be sub-populations of cancer cells where mitotic failure ultimately does not lead to mitotic catastrophe. As a consequence, extensively altered genomes could be induced. These might provoke resistance towards therapy because death signals can no longer rely on functioning pathways (Holland and Cleveland 2014). Correspondingly, centrosomal amplification resulting from CFI treatment is linked

to tumorigenesis, so there might be an increased risk of tumor progression under therapy (Holland and Cleveland 2014).

5.3.3 Reasons for a combined use of CFI and MK2 inhibitor versus single-use of CFI

One might argue that CFI on its own might be enough of treatment – it causes replicative stress *and* abolishes the SAC, this way provoking mitotic failure and catastrophe. Why is an additional drug, namely an MK2 inhibitor (that even takes out some of the stress that is caused by PLK4 inhibition) necessary? Firstly, literature demonstrates that MK2 inhibition leads to impairment of the G2/M checkpoint (Manke et al. 2005). Secondly, we showed in 4.2 that additional MK2 inhibition leads to a further reduction of cell proliferation. Thus, one may conclude that the abolishment of an additional checkpoint is in this case more essential in combating cancer cells than the further enhancement of replicative stress.

5.3.4 Combined treatment with AURKB inhibitor and MK2 inhibitor

Given that the replicative stress caused by CFI is mostly rescued by MK2 inhibition, it would be conceivable that replicative stress is not the lethal function of CFI in this context. In fact, AURKB inhibition might be even more essential. In order to prevent the patient from overmedication, it needs to be examined whether the simpler combination of AURKB inhibitor and MK2 inhibitor might be similarly effective as the combination of CFI and MK2 inhibitor. This would need to be tested experimentally.

5.4 What remains to be done?

Although the combination of CFI and an MK2 inhibitor seems tempting, our experiments only provide the first hint regarding its possible efficacy in tumor treatment.

5.4.1 Recovery of cancer cells after shorter treatment

The *Celigo* experiments with combined CFI and MK2 inhibition were carried out under continuous treatment of the cells over the whole period of the experiment. Transferred to clinical routine, this would imply permanent medication until the

end of a patient's life. Certainly, this does not represent a desired scenario. Severe side-effects may be anticipated when interfering with mechanisms vivid in all somatic cells like DNA replication and cell cycle regulation. Thus, our cell proliferation assays need to be repeated, this time with a treatment for several days – until an effect is visible – and a wash-out of the treatments after this period. This would reveal whether cells are truly irrevocably destroyed or whether they recover after a short amount of time.

5.4.2 The affection of healthy tissue by the drugs

Furthermore, the affection of healthy tissue would need to be evaluated. Checkpoints and DNA replication are essential in every kind of cell. So how can healthy cells survive while cancer cells are targeted? The fact that replicative stress is endogenously enhanced in cancer cells and PLK4 levels are elevated in many kinds of tumors suggests that there might be a certain inherent specificity of CFI towards tumor cells. Apart from that, the p53 status of a tumor might play an important role. Wild-type p53 could compensate for the other defective checkpoints caused by combined CFI and MK2 inhibitor treatment (SAC and G2/M checkpoint).

As explained above, mutant p53 cells have an endogenously abolished G1/S checkpoint. On top of the inactivation of G2/M this probably contributes to the mitotic catastrophe taking place in these cells. It remains to be elucidated whether cells with wild-type p53 and thus with proficient G1/S and G2/M checkpoints are more resistant towards treatment with CFI and MK2 inhibitor. Therefore, our experiments would need to be repeated in different p53 mutant and p53 wild-type (non-cancer) cell lines.

Interestingly, experiments with CFI were already performed in Ewing's sarcoma and different lung cancer cell lines, showing no influence of the p53 status of the cell line on cell survival following CFI treatment (Kawakami et al. 2018a; Kerschner-Morales et al. 2020)

5.4.3 Evolving biomarkers and testing in xenografts

Not all tumors are prone towards the same medication. In the last years, progress has been made by identifying biomarkers that predict a tumor's susceptibility to

a certain drug. For combined CFI and MK2 inhibitor treatment, the p53 status could act as a biomarker and a predictor of sensitivity towards the treatment. Furthermore, PLK4 levels might serve as a prognostic marker of susceptibility towards CFI treatment. This has been postulated by other authors who found PLK4 levels elevated in different types of tumors (compare 1.1.3.2).

Bringing the experiments to the next level, the combination of drugs would need to be tested in tumor xenografts. Following that, a clinical level could be reached and eventually patients could be treated.

6 Abstract

Cancer cells are prone to replicative stress to a greater extent than healthy cells are. Thus, replicative stress might be a way to target cancer cells in a more specific way than conventional chemotherapeutics do. According to previous results, one way to exert replicative stress on cells is the inhibition of the centrosomal protein Polo-like kinase 4 (PLK4).

The small compound CFI-400945 is a PLK4 inhibitor. CFI-400945 is currently being tested in phase I and II clinical trials, still its mechanisms of action partly remain elusive. Therefore, we examined the effect of CFI-400945 on DNA replication and cell proliferation in H1299 cells, with methods including cell microscopy, DNA fiber assays, western blot analyses, flow cytometry and immunofluorescence. As a result, we found that CFI-400945 manages to reduce the proliferation of cells by two means: Firstly by the exertion of replicative stress through the p38-MK2 signaling pathway and secondly by the induction of mitotic failure and mitotic catastrophe. The number of centrosomes in our experiments was affected in an unexpected way: In response to CFI-400945 treatment, we observed amplification of centrosomes – an effect that cannot be recapitulated by PLK4 knockdown. This strongly indicates an off-target effect executed by CFI-400945. As it is mechanistically conceivable, supported by literature and suggested by further experiments, we propose that it is Aurora kinase B inhibition that contributes to the effects of CFI-400945.

The additional Aurora kinase B inhibition by CFI-400945 would also explain the synergistic cell lethality that we observed with combined CFI-400945 and MK2 inhibitor treatment. Although replication fork progression was rescued partly by the additional MK2 inhibitor treatment, the cell proliferation was reduced even more than with single CFI-400945 treatment. We propose that this can be explained by the combination of enhanced DNA replication and ablation of cell cycle checkpoints. Combined targeting of checkpoints governing DNA replication and mitosis might prove to represent a viable strategy of eliminating cancer cells.

7 Deutsche Zusammenfassung

Krebszellen sind anfälliger für replikativen Stress als gesunde Zellen. Aus diesem Grund könnte replikativer Stress ein möglicher Angriffspunkt sein, um Krebszellen auf eine selektivere Art zu schädigen als mit konventionellen Chemotherapeutika. Bisherige Ergebnisse unserer Arbeitsgruppe zeigen, dass die Inhibition des zentrosomalen Proteins PLK4 (*Polo-like kinase 4*) eine Möglichkeit darstellt, replikativen Stress auf Zellen auszuüben.

Der *small molecule inhibitor* CFI-400945 ist ein PLK4-Inhibitor. CFI-400945 wird derzeit in klinischen Studien der Phase I und II getestet, jedoch sind seine Wirkungsmechanismen noch nicht vollständig geklärt. Daher untersuchten wir die Wirkung von CFI-400945 auf DNA-Replikation und Zellproliferation in H1299-Zellen. Methodisch wurden Zellmikroskopie, *DNA fiber assays*, Western Blot-Analysen, Durchflusszytometrie und Immunfluoreszenz angewandt. Als Ergebnis stellten wir fest, dass CFI-400945 die Zellproliferation auf zwei Arten reduziert: zum einen durch die Ausübung von replikativem Stress über den p38-MK2-Signalweg und zum anderen durch die Induktion von Mitoseversagen und mitotischer Katastrophe. Die Anzahl der Zentrosomen wurde durch CFI-400945 in unseren Experimenten in unerwarteter Weise beeinflusst: Als Reaktion auf die Behandlung mit CFI-400945 beobachteten wir eine Amplifikation der Zentrosomen - ein Effekt, der durch den Knockdown von PLK4 nicht rekapituliert werden kann. Dies deutet auf einen durch CFI-400945 ausgeübten Off-Target-Effekt hin. Da ein solcher Off-Target-Effekt aus mechanistischer Sicht plausibel ist und von der Literatur sowie von weitergehenden Experimenten unterstützt wird, vermuten wir, dass die Hemmung der Aurora-B-Kinase zu den Effekten von CFI-400945 beiträgt.

Die zusätzliche Hemmung der Aurora-B-Kinase durch CFI-400945 würde auch die synergistische Zellletalität erklären, die wir bei der kombinierten Behandlung mit CFI-400945 und MK2-Inhibitoren beobachtet haben. Obwohl das Fortschreiten der Replikationsgabel durch die zusätzliche Behandlung mit dem MK2-Inhibitor teilweise wiederhergestellt werden konnte, war die Zellproliferation sogar noch stärker reduziert als bei einer alleinigen Behandlung mit CFI-400945. Wir vermuten, dass dies anhand der Kombination von gesteigerter DNA-Replikation und Ablation von Zellzyklus-Kontrollpunkten erklärt werden kann.

Das kombinierte Abschalten dieser Kontrollpunkte, die die DNA-Replikation einerseits und die Mitose andererseits regulieren, könnte sich als tragfähige Strategie zur Eliminierung von Krebszellen erweisen.

8 References

Bartek J, Lukas C, Lukas J (2004): Checking on DNA damage in S phase. Nat Rev Mol Cell Biol 5, 792–804

Carmena M, Earnshaw WC (2003): The cellular geography of aurora kinases. Nat Rev Mol Cell Biol 4, 842–854

Castedo M, Perfettini JL, Roumier T, Andreau K, Medema R, Kroemer G (2004): Cell death by mitotic catastrophe: a molecular definition. Oncogene 23, 2825–2837

Collins I, Garrett MD (2005): Targeting the cell division cycle in cancer: CDK and cell cycle checkpoint kinase inhibitors. Curr Opin Pharmacol 5, 366–373

Cooper GM, Hausman RE: The cell: a molecular approach. 7th Edition; Sinauer Associates, Oxford 2015

Coudreuse D, Nurse P (2010): Driving the cell cycle with a minimal CDK control network. Nature 468, 1074–1079

Dammermann A, Müller-Reichert T, Pelletier L, Habermann B, Desai A, Oegema K (2004): Centriole assembly requires both centriolar and pericentriolar material proteins. Dev Cell 7, 815–829

Dobbelstein M, Sørensen CS (2015): Exploiting replicative stress to treat cancer. Nat Rev Drug Discov 14, 405–423

Donzelli M, Draetta GF (2003): Regulating mammalian checkpoints through Cdc25 inactivation. EMBO Rep 4, 671–677

Eichenauer DA, Aleman BMP, André M, Federico M, Hutchings M, Illidge T, Engert A, Ladetto M (2018): Hodgkin lymphoma: ESMO Clinical Practice Guidelines for diagnosis, treatment and follow-up. Ann Oncol 29 Suppl 4, iv19-iv29

Habedanck R, Stierhof YD, Wilkinson CJ, Nigg EA (2005): The Polo kinase Plk4 functions in centriole duplication. Nat Cell Biol 7, 1140–1146

Holland AJ, Cleveland DW (2014): Polo-like kinase 4 inhibition: a strategy for cancer therapy? Cancer Cell 26, 151–153

Kawabe T (2004): G2 checkpoint abrogators as anticancer drugs. Mol Cancer Ther 3, 513–519

Kawakami M, Mustachio LM, Zheng L, Chen Y, Rodriguez-Canales J, Mino B, Kurie JM, Roszik J, Villalobos PA, Thu KL et al. (2018a): Polo-like kinase 4

inhibition produces polyploidy and apoptotic death of lung cancers. Proc Natl Acad Sci U S A 115, 1913–1918

Kawakami M, Mustachio LM, Zheng L, Chen Y, Rodriguez-Canales J, Mino B, Kurie JM, Roszik J, Villalobos PA, Thu KL et al. (2018b): Reply to Oegema et al.: CFI-400945 and Polo-like kinase 4 inhibition. Proc Natl Acad Sci U S A 115, E10810-E10811

Kazazian K, Go C, Wu H, Brashavitskaya O, Xu R, Dennis JW, Gingras AC, Swallow CJ (2017): Plk4 promotes cancer invasion and metastasis through Arp2/3 complex regulation of the actin cytoskeleton. Cancer Res 77, 434–447

Kelleher FC, Kroes J, Lewin J (2019): Targeting the centrosome and polo-like kinase 4 in osteosarcoma. Carcinogenesis 40, 493-499

Kerschner-Morales SL, Kühne M, Becker S, Beck JF, Sonnemann J (2020): Anticancer effects of the PLK4 inhibitors CFI-400945 and centrinone in Ewing's sarcoma cells. J Cancer Res Clin Oncol 146, 2871–2883

Labianca R, Nordlinger B, Beretta GD, Mosconi S, Mandalà M, Cervantes A, Arnold D (2013): Early colon cancer: ESMO Clinical Practice Guidelines for diagnosis, treatment and follow-up. Ann Oncol 24 Suppl 6, vi64-72

Levine MS, Bakker B, Boeckx B, Moyett J, Lu J, Vitre B, Spierings DC, Lansdorp PM, Cleveland DW, Lambrechts D et al. (2017): Centrosome amplification is sufficient to promote spontaneous tumorigenesis in mammals. Dev Cell 40, 313-322.e5

Lohse I, Mason J, Cao PM, Pintilie M, Bray M, Hedley DW (2017): Activity of the novel polo-like kinase 4 inhibitor CFI-400945 in pancreatic cancer patient-derived xenografts. Oncotarget 8, 3064–3071

Luo Y, Barrios-Rodiles M, Gupta GD, Zhang YY, Ogunjimi AA, Bashkurov M, Tkach JM, Underhill AQ, Zhang L, Bourmoum M et al. (2019): Atypical function of a centrosomal module in WNT signalling drives contextual cancer cell motility. Nat Commun 10, 2356

Manke IA, Nguyen A, Lim D, Stewart MQ, Elia AEH, Yaffe MB (2005): MAPKAP kinase-2 is a cell cycle checkpoint kinase that regulates the G2/M transition and S phase progression in response to UV irradiation. Mol Cell 17, 37–48

Mason JM, Lin DC-C, Wei X, Che Y, Yao Y, Kiarash R, Cescon DW, Fletcher GC, Awrey DE, Bray MR et al. (2014): Functional characterization of CFI-400945, a Polo-like kinase 4 inhibitor, as a potential anticancer agent. Cancer Cell 26, 163–176

Morgan DO (1997): Cyclin-dependent kinases: engines, clocks, and microprocessors. Annu Rev Cell Dev Biol 13, 261–291

Moyer TC, Clutario KM, Lambrus BG, Daggubati V, Holland AJ (2015): Binding of STIL to Plk4 activates kinase activity to promote centriole assembly. J Cell Biol 209, 863–878

Nakamura T, Saito H, Takekawa M (2013): SAPK pathways and p53 cooperatively regulate PLK4 activity and centrosome integrity under stress. Nat Commun 4, 1775

Nam HJ, Naylor RM, van Deursen JM (2015): Centrosome dynamics as a source of chromosomal instability. Trends Cell Biol 25, 65–73

Oegema K, Davis RL, Lara-Gonzalez P, Desai A, Shiau AK (2018): CFI-400945 is not a selective cellular PLK4 inhibitor. Proc Natl Acad Sci U S A 115, E10808-E10809

Passerini V, Ozeri-Galai E, de Pagter MS, Donnelly N, Schmalbrock S, Kloosterman WP, Kerem B, Storchová Z (2016): The presence of extra chromosomes leads to genomic instability. Nat Commun 7, 10754

Press MF, Xie B, Davenport S, Zhou Y, Guzman R, Nolan GP, O'Brien N, Palazzolo M, Mak TW, Brugge JS et al. (2019): Role for polo-like kinase 4 in mediation of cytokinesis. Proc Natl Acad Sci U S A 116, 11309–11318

Reinhardt HC, Hasskamp P, Schmedding I, Morandell S, van Vugt MATM, Wang X, Linding R, Ong SE, Weaver D, Carr SA et al. (2010): DNA damage activates a spatially distinct late cytoplasmic cell-cycle checkpoint network controlled by MK2-mediated RNA stabilization. Mol Cell 40, 34–49

Renart J, Reiser J, Stark GR (1979): Transfer of proteins from gels to diazobenzyloxymethyl-paper and detection with antisera: a method for studying antibody specificity and antigen structure. Proc Natl Acad Sci U S A 76, 3116–3120

Rosario CO, Kazazian K, Zih FSW, Brashavitskaya O, Haffani Y, Xu RSZ, George A, Dennis JW, Swallow CJ (2015): A novel role for Plk4 in regulating cell spreading and motility. Oncogene 34, 3441–3451

Roth GA, Abate D, Abate KH, Abay SM, Abbafati C, Abbasi N, Abbastabar H, Abd-Allah F, Abdela J, Abdelalim A et al. (2018): Global, regional, and national age-sex-specific mortality for 282 causes of death in 195 countries and territories, 1980-2017: a systematic analysis for the Global Burden of Disease Study 2017. Lancet 392, 1736–1788

Shapiro AL, Viñuela E, Maizel Jr JV (1967): Molecular weight estimation of polypeptide chains by electrophoresis in SDS-polyacrylamide gels. Biochem Biophys Res Commun 28, 815–820

Shinmura K, Kurabe N, Goto M, Yamada H, Natsume H, Konno H, Sugimura H (2014): PLK4 overexpression and its effect on centrosome regulation and chromosome stability in human gastric cancer. Mol Biol Rep 41, 6635–6644

Smith PK, Krohn RI, Hermanson GT, Mallia AK, Gartner FH, Provenzano MD, Fujimoto EK, Goeke NM, Olson BJ, Klenk DC (1985): Measurement of protein using bicinchoninic acid. Anal Biochem 150, 76–85

Smith SL, Bowers NL, Betticher DC, Gautschi O, Ratschiller D, Hoban PR, Booton R, Santibáñez-Koref MF, Heighway J (2005): Overexpression of aurora B kinase (AURKB) in primary non-small cell lung carcinoma is frequent, generally driven from one allele, and correlates with the level of genetic instability. Br J Cancer 93, 719–729

Sredni ST, Suzuki M, Yang JP, Topczewski J, Bailey AW, Gokirmak T, Gross JN, de Andrade A, Kondo A, Piper DR et al. (2017): A functional screening of the kinome identifies the Polo-like kinase 4 as a potential therapeutic target for malignant rhabdoid tumors, and possibly, other embryonal tumors of the brain. Pediatr Blood Cancer 64, e26551

Stegmann K: Combined inhibition of protein kinases to interfere with centrosome integrity and mitosis of cancer cells. Unpublished master's thesis (Molecular Medicine) Göttingen 2019

Su CC, Chen NC, Chyau CC, Tseng HC, Chou FP (2018): Induction of mitotic catastrophe via inhibition of Aurora B by ionizing radiation with additive of mulberry water extract in human bladder cancer cells. Integr Cancer Ther 18, 1534735418808586

Suri A, Bailey AW, Tavares MT, Gunosewoyo H, Dyer CP, Grupenmacher AT, Piper DR, Horton RA, Tomita T, Kozikowski AP et al. (2019): Evaluation of Protein Kinase Inhibitors with PLK4 Cross-Over Potential in a Pre-Clinical Model of Cancer. Int J Mol Sci 20, 2112

Tao Y, Leteur C, Calderaro J, Girdler F, Zhang P, Frascogna V, Varna M, Opolon P, Castedo M, Bourhis J et al. (2009): The aurora B kinase inhibitor AZD1152 sensitizes cancer cells to fractionated irradiation and induces mitotic catastrophe. Cell Cycle 8, 3172–3181

Tayeh Z.: Centrosome integrity as a determinant of replication stress. Dissertation (Molecular Medicine) Göttingen 2019

Tayeh Z, Stegmann K, Kleeberg A, Friedrich M, Choo JAMY, Wollnik B, Dobbelstein M (2020): Centrosome impairment causes DNA replication stress through MLK3/MK2 signaling and R-loop formation. [unpublished manuscript under consideration; submitted as a preprint paper to bioRxiv 2020.01.09.898684; doi: https://doi.org/10.1101/2020.01.09.898684]

Thornton TM, Rincon M (2009): Non-Classical P38 Map Kinase Functions: Cell Cycle Checkpoints and Survival. Int J Biol Sci 5, 44–51

Thorpe GH, Kricka LJ (1986): Enhanced chemiluminescent reactions catalyzed by horseradish peroxidase. Meth Enzymol 133, 331–353

Tian X, Zhou D, Chen L, Tian Y, Zhong B, Cao Y, Dong Q, Zhou M, Yan J, Wang Y et al. (2018): Polo-like kinase 4 mediates epithelial-mesenchymal transition in neuroblastoma via PI3K/Akt signaling pathway. Cell Death Dis 9, 54

Towbin H, Staehelin T, Gordon J (1979): Electrophoretic transfer of proteins from polyacrylamide gels to nitrocellulose sheets: procedure and some applications. Proc Natl Acad Sci U S A 76, 4350–4354

Veitch ZW, Cescon DW, Denny T, Yonemoto LM, Fletcher G, Brokx R, Sampson P, Li S-W, Pugh TJ, Bruce J et al. (2019): Safety and tolerability of CFI-400945, a first-in-class, selective PLK4 inhibitor in advanced solid tumours: a phase 1 dose-escalation trial. Br J Cancer 121, 318–324

Walworth NC (2000): Cell-cycle checkpoint kinases: checking in on the cell cycle. Curr Opin Cell Biol 12, 697–704

Wong YL, Anzola JV, Davis RL, Yoon M, Motamedi A, Kroll A, Seo CP, Hsia JE, Kim SK, Mitchell JW et al. (2015): Cell biology. Reversible centriole depletion with an inhibitor of Polo-like kinase 4. Science 348, 1155–1160

Yasutis KM, Kozminski KG (2013): Cell cycle checkpoint regulators reach a zillion. Cell Cycle 12, 1501–1509

Zhang Z, Wang Z, Huang K, Liu Y, Wei C, Zhou J, Zhang W, Wang Q, Liang H, Zhang A et al. (2019): PLK4 is a determinant of temozolomide sensitivity through phosphorylation of IKBKE in glioblastoma. Cancer Lett 443, 91–107

Acknowledgements

First of all, I would like to express my gratitude to my doctoral thesis advisor *Prof. Dr. Matthias Dobbelstein*, for giving me the opportunity to conduct my doctoral thesis in his group and for his extensive guidance throughout the project. The weekly meetings and his continuous accessibility were a unique support.

Also, I would like to thank *Prof. Dr. Elisabeth Heßmann,* who kindly agreed to be my second thesis committee member, for investing time and giving important feedback.

Thank you to my internal supervisor *Dr. Zainab Tayeh* who taught me the laboratory techniques needed in my experiments. Her constant support was very helpful.

In this context, I would also like to mention the entire *Institute of Molecular Oncology*. Thanks to everyone for being supportive and promoting a cooperative working environment.

My academic studies were supported by the *Studienstiftung des deutschen Volkes* whom I want to thank for their financial and ideal support.

Thank you to *Tilman Horn* for being a critical corrector as well as a very supportive mind throughout my doctoral thesis.

Last but definitely not least, my gratitude goes to *Karen Iversen-Kleeberg* and *Jürgen Kleeberg*. Thank you for your constant support and encouragement.